FMG based continuous finger movement prediction toward partial hand prosthesis control

by

Rana Sadeghi Chegani

B.Sc., Amirkabir University of technology, 2015

Thesis Submitted in Partial Fulfillment of the
Requirements for the Degree of
Master of Applied Science

in the
School of Engineering Science
Faculty of Applied Science

SIMON FRASER UNIVERSITY
Fall 2018

Approval

Name:	**Rana Sadeghi Chegani**
Degree:	**Master of Applied Science (Biomedical Engineering)**
Title:	**FMG based continuous finger movement prediction toward partial hand prosthesis control**
Examining Committee:	**Chair:** Steve Whitmore Senior Lecturer
	Carlo Menon Senior Supervisor Professor
	Edward Jung Wook Park Supervisor Professor
	Faranak Farzan Internal Examiner Assistant Professor School of Mechatronic Systems Engineering
Date Defended:	**December 10, 2018**

Ethics Statement

The author, whose name appears on the title page of this work, has obtained, for the research described in this work, either:

a. human research ethics approval from the Simon Fraser University Office of Research Ethics

or

b. advance approval of the animal care protocol from the University Animal Care Committee of Simon Fraser University

or has conducted the research

c. as a co-investigator, collaborator, or research assistant in a research project approved in advance.

A copy of the approval letter has been filed with the Theses Office of the University Library at the time of submission of this thesis or project.

The original application for approval and letter of approval are filed with the relevant offices. Inquiries may be directed to those authorities.

Simon Fraser University Library
Burnaby, British Columbia, Canada

Update Spring 2016

Abstract

Partial hand amputation forms more than 90% of all the upper limb amputations. To improve the quality of life for partial hand amputees different prosthesis options, including externally-powered prosthesis, have been investigated. This work is exploring Force Myography (FMG) as a technique for regressing grasping movement accompanied by wrist position variations. This study can lay the groundwork for a future investigation of FMG as a technique for controlling externally-powered prostheses continuously. Ten able-bodied participants performed three hand movements while their wrist was fixed in one of the six predefined positions. Two approaches were examined for estimating grasping: (i) one regression model, trained on data from all wrist positions and hand movements; (ii) a classifier that identified the wrist position followed by a separate regression model for each wrist position. Both approaches presented similar performance while the first approach was more than two times faster. The results indicate the potential of FMG to regress grasping movement, accompanied by wrist position variations.

Keywords: Force Myography; Random forest; Continuous grasping predication; Partial hand prosthesis; Finger movement prediction

Dedication

I would like to dedicate this thesis to those whom work hard to help individuals with an amputation fulfill their potential.

Acknowledgements

Firstly, I like to thank my senior supervisor, Dr. Carlo Menon for his guidance and support throughout my research.

Moreover, I like to thank the past and present members of MENRVA research group, for their valuable supported during my research. I specially like to thank Dr. Zhen Xiao for his guidance thought the course of my work.

Also, I like to acknowledge Dr. Carolyn Sparrey, for her cooperation and assistance during the research.

Last and not least, I am thankful to all my friends and family who supported me by taking time and participating in my experiment and providing me feedback. Specially my husband for his tremendous support and help during my masters.

Table of Contents

List of Tables

List of Figures

Chapter 1

Introduction

3.6 million people are expected to live with an amputation by 2050 [1]. Historical data show that approximately 35% of amputations are related to the upper extremity [1]. The upper limb amputation can be categorized into two categories based on the level of the amputation. An amputation above or below the elbow is defined as a *major upper-limb loss*. The *minor upper-limb loss* or *partial hand amputation* is defined as amputation of digits, or hands. The majority of the upper limb amputations (i.e. over 90%) are partial hand amputations [1]. Partial hand amputation, can impose a notable influence on a person's life. It can have an adverse effect on their self-image, can cause loss of job and emotional distress [2]. Epidemiological studies show that the number of partial hand amputations per year is one every 18,000-20,000 residents [3]. A 2018 report indicates that there were 209,053 hospital visits specifically related to hand and digit injuries between 2002 and 2010, and 5000 work-related finger amputations in 2010 in the United States alone [4].

Although the minor upper-limb amputation is a common injury (due to the vulnerability of the fingers), the research in the field of partial hand amputation has moderately progressed compared to the research in major upper limb amputation filed [5, 3]. One of the main reasons is the high variability of the amputation level and shape, which can be unique to the individual [5, 6].

Partial hand amputation can lead to losing the functionality of the upper limb drastically. We use our hands for a variety of tasks in our daily routine. Amputation of all the fingers and thumb through Metacarpophalangeal (MCP) joints results in 54% impairment rating of the body as a whole, while it results in 90% impairment of the upper limb

[7]. Amputation of the thumb through MCP joints results in 40% impairment rate of the hand, 36% impairment of the upper extremity, and 22% impairment of the body [7]. The impairment rate emphasizes the effect of the partial hand amputation on the functionality of the body. One solution to resolve some of the problems regarding the amputation is to fit partial hand amputees with a prosthesis [3]. Often partial hand amputees are not able to go back to the same job after amputation, and based on their job they may not find a prosthesis useful [8]. This points out the importance of providing a functional prosthesis for individuals with partial hand amputations. The prosthesis options for partial hand amputees can be categorized as the passive or active prosthesis. Figure 1.1 shows a diagram of different categories of partial prosthetic hands. The passive prosthesis is either used for cosmetic appearance, or as prosthetic tools. The cosmetic prosthesis tries to resemble the skin color and look of the real hand (Figure 1.1.a). The prosthetic tools can be designed for different activities, such as hammering a nail, playing an instrument, or playing different sport (Figure 1.1.b)[9]. The active prosthesis can be classified into body-powered partial hand prosthesis and externally-powered partial hand prosthesis. The body-powered partial hands can use the shoulder, wrist, finger residuals or remaining fingers to control the prosthesis, depending on the level of the amputation. Using shoulder for controlling partial hand prosthesis is not as common since it does not look natural and it needs complicated shoulder movement for controlling (Figure 1.1.c). The wrist-powered prosthesis is more suitable for users who lost all the fingers without any finger residuals that can control the prosthesis (Figure 1.1.d). The drawback of wrist-powered prostheses is that often all the fingers are controlled together, and this limits the user to open and close grasps. The finger-powered prostheses are suitable for the users who lost a portion of the finger and have at least the metacarpophalangeal joints (MCP) attached (Figure 1.1.e). These prostheses use the finger residual to control the prosthesis [10].

The externally-powered partial hand prostheses, use biosignals from the user to control the hand [11]. Biosignal can be defined as any continuous signal that is recorded from a living being. The commercially available devices often use the signal from the muscles. Currently, there are two externally-powered partial hand prosthesis available in the market (Figure

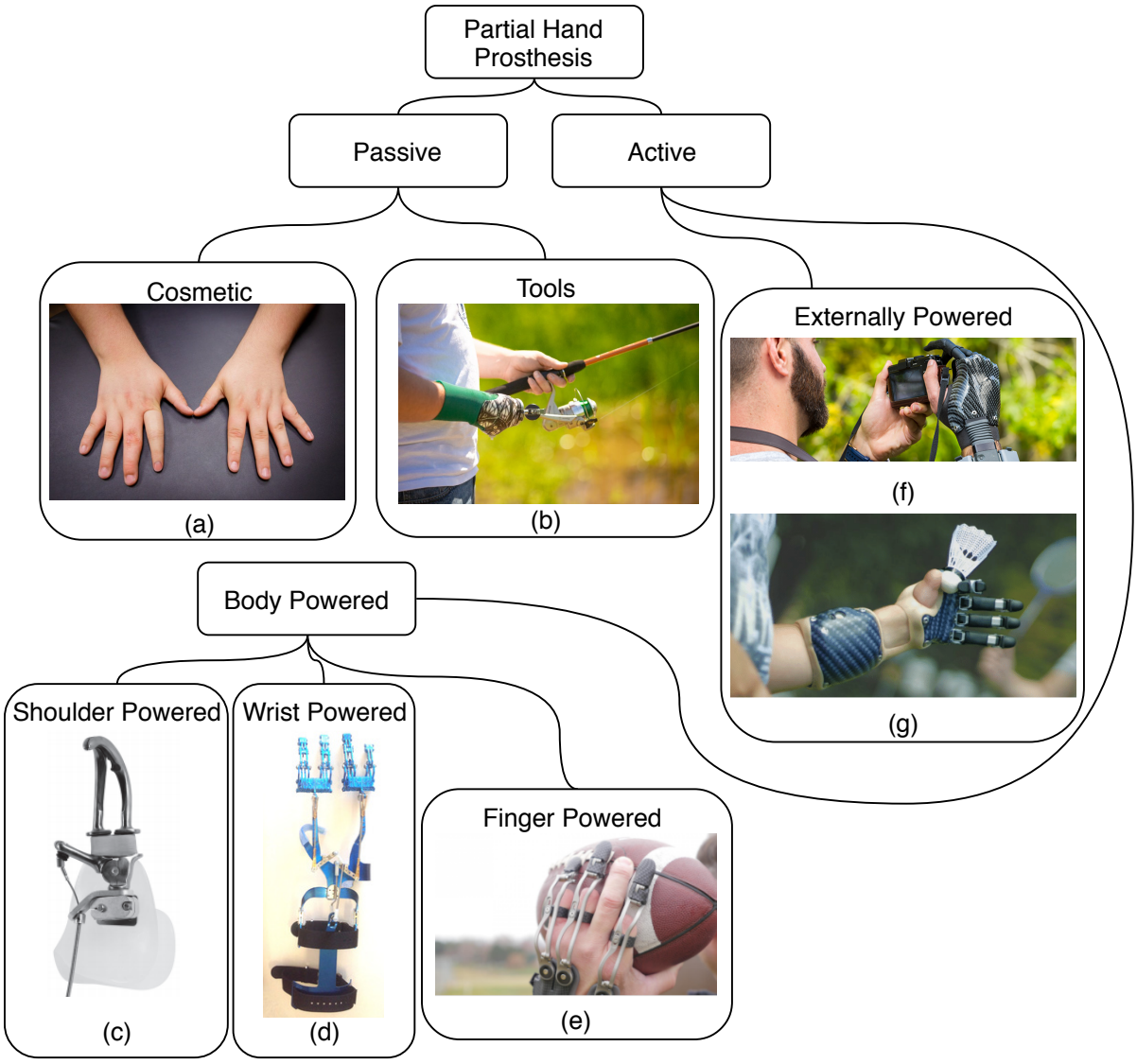

Figure 1.1: a. Cosmetic prosthesis b. Prosthetic tools c. Shoulder powered prosthesis d. Wrist powered prosthesis e. Finger powered prosthesis f. i-digit by touch bionics g. VINCENTpartial by Vincent Systems [1]

1.1.f and Figure 1.1.g). The *i-digit* from touch bionics by Ossur [2] and *VINCENTpartial*

[1] a & b. https://www.armdynamics.com/our-care/finger-and-partial-hand-prosthetic-options;
c. http://www.hosmer.com;
d. http://www.x-finger.com;
e. http://www.npdevices.com
f. https://www.touchbionics.com;
g. https://vincentsystems.de/en

[2]https://www.touchbionics.com

from Vincent systems[3]. The *i-digit* uses the surface Electromyography (sEMG) from the user's wrist to control the hand. The *VINCENTpartial* prosthesis uses sEMG, touch pads, bend sensors or a combination of them to control the hand. Both of the products use pattern recognition approach to control their device. In the pattern recognition approach, the biosignal from the user is mapped to a set of specific pre-programmed hand gestures. With proper sensor placement and training, the user can control the hand to shape one of the pre-programmed hand gestures. Although this pattern recognition approach can achieve a high classification accuracy, it limits the user to some specific hand gestures [12].

It is essential to keep in mind that each of the prostheses options have their pros and cons. The rehabilitation team can provide an optimized solution for the amputee with careful considerations of the amputee's needs. An individual may need to use a combination of the options to achieve satisfaction [11].

Regarding the externally powered prosthesis, the limitations about the number of the grasps that an individual can perform motivated us to investigate Force Myography (FMG) for continuous hand movement prediction. This can potentially lead to continuous finger movement control of the prosthesis. FMG is defined as tracking the volumetric changes in a muscle associated with the muscles contraction or relaxation during the functional movement of the limb [13].

In partial hand amputees with a functional wrist, the intention to perform a hand grasp (either with remaining digits or to control a prosthesis) is accompanied with wrist movement. The forearm and wrist include the tendons and muscles that control both wrist and digits. The biosignal from the forearm and wrist muscles and tendons carry information from the movement of both wrist and digits. As mentioned earlier, the commercially available externally-powered prosthesis uses the biosignal from the user's forearm and wrist to control the prosthesis. If the control system of the prosthesis is trained on a specific wrist position, the movement of the wrist during the prosthesis usage can have an adverse effect on the control system's performance [14, 15].

[3]https://vincentsystems.de/en

The effect of the wrist movement on the biosignal provided the second motivation of this work. Therefore, the effect of the wrist movement during grasping movement prediction using the FMG signal was explored.

1.1 Objectives and hypothesis

In the present work, inspired by the limitations mentioned in the currently available partial hand prosthesis, the following objectives were established (as this is a preliminary research able-bodied participants were used for data collection):

Objective 1. Explore different regression models for continuous hand movement prediction and different classification models for wrist position classification using FMG signal. In addition, validate the usage of FMG signal for continuous hand movement prediction

Objective 2. Investigate the effect of the wrist position on the prediction and the possibility of reducing the number of the wrist positions during training

The fundamental hypothesis of this work is that the FMG signal can predict continuous hand movements, in the presence of wrist position variation.

It is important to remind that although the study has not been tested on the amputees, the study of the signal from healthy individuals can provide the groundwork for a further study on the amputees in future research.

1.2 Thesis structure

The remainder of the thesis is structured as follows:

- In Chapter 2, first an overview of the anatomy of the hand and wrist is provided. The anatomy of the limb can help to identify a data collection location of the limb that provides valuable information on the fingers and wrist movement. In addition to that, the related works in the field of the externally powered-prosthesis control and effect of the wrist movement on the biosignal are reviewed in this chapter. The presented review helps to identify the machine learning algorithms to explore to meet **objective 1**.

- Chapter 3 provides information and examples on the machine learning algorithms that have been used with FMG before. This includes linear classification, linear regression, Support Vector Machine, and Neural Network. In additional to conventional machine learning algorithms, Random Forest (RF) is introduced in this chapter. The explained machine learning algorithms will be explored later on, to cover **objective 1**.

- The setup and protocol of the experiment are provided in Chapter 4. More specifically, the design of the data collection band, experimental protocol, data collection software, selected grasp types and wrist positions, and processing of the hand motion data are covered in this chapter. The setup and protocol are designed to collect data which can be analyzed toward covering objective 1 and objective 2.

- Chapter 5 explains the analysis of the motion data, and FMG data to cover **objective 1**. In this chapter different machine learning algorithms are explored for both regression and classification. The exploration and comparison between different machine learning algorithms help to identify the proper algorithm, for the continuous hand movement prediction in this work. The result of comparison helps to validate the possibility of using FMG signal for hand movement regression in different wrist positions.

- Chapter 6 covers **objective 2**. The chapter investigates the effect of wrist position on the FMG data. Moreover, the result of this chapter can identify whether it's possible to reduce the time and size of the training data collection.

- Chapter 7 presents a conclusion of finding and outlines how each objective was met. In addition, it covers suggestions for future investigations.

Chapter 2

Background

In this chapter, a brief background about the wrist, and forearm anatomy and a literature review of the existing methods for finger movement estimation and continuous hand movement prediction is presented. The literature review presented in this chapter helps to identify different regression models and hand movements that have been used, especially with FMG signal, for continuous hand movement prediction. The review presented in 2.2.1 can provide information to recognize which classification and regression models should be explored to meet **objective 1**.

2.1 Wrist, and forearm anatomy

Figure 2.1 indicates the bones and joints of the hand. Based on the information presented in the figure, the finger joints will be referred to as DIP, PIP, and MCP, and the joints of the thumb will be referred to as IP and MCP throughout the manuscript.

Figure 2.2 indicates the muscles and tendons in the forearm and wrist. Based on the location of the muscles and tendons relative to the skin, they can be categorized as *Superficial* or *Deep*. Superficial muscles are near the skin surface, deep muscles are further from the skin surface and near the internal center of the limb [16].

The muscles controlling the wrist and digits are listed in Table 2.1 [16]. These muscles are responsible for the wrist, finger, and thumb movements. These movements include Flexion, Extension, Abduction, and Adduction. Flexion is bending or decreasing the angle between bones or parts of the body, like bending the elbow joint. An extension is the movement opposite to flexion and is the straightening of the joints of the body. Abduction means

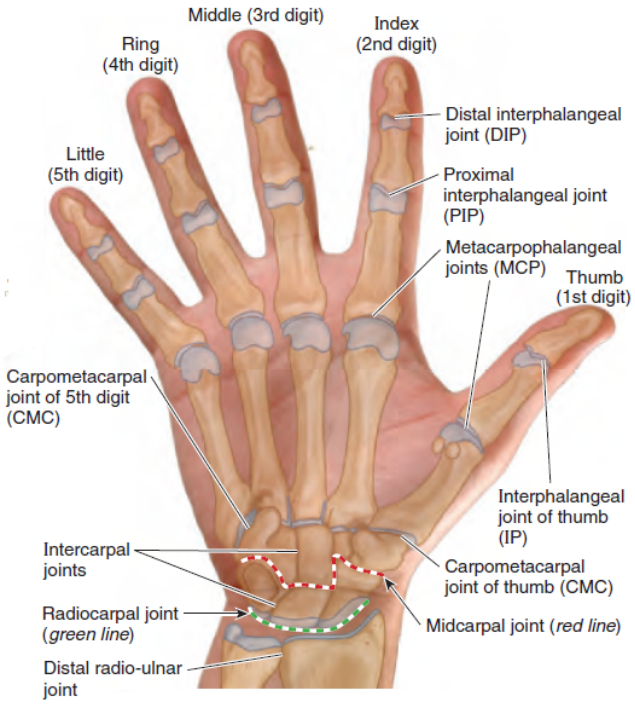

Figure 2.1: The bones and joints of hand [17]

moving a part of the body away from the middle, like moving the upper limb away from the body. Adduction is the opposite of abduction [16]. As the table indicates, all of the wrist-controlling muscles are superficial, all of the thumb-controlling muscles are deep, and half of the finger controlling muscles are superficial, the other half are located deep under the surface of the skin.

As Figure 2.2 indicates, by moving toward the wrist, some of the finger controlling and thumb controlling muscles become closer to the skin surface. For instance, the Extensor Pollicis Longus (EPL) muscle, which is responsible for extending the MCP joints, is surrounded by Extensor Carpi Ulnaris (ECU) and Extensor Pollicis Brevis (EPB) in the mid-forearm, while it is closer to the skin surface near the wrist. The Flexor Pollicis Longus (FPL) muscle, which is responsible for flexing the thumb, is enveloped by Flexor Digitorum Superficial (FDS) and Flexor Digitorum Profundus (FDP), near the wrist it is closer to the skin surface; the Extensor Indicis Proprius (EIP) muscle, responsible for extending the index finger, starts below the mid-forearm. As a result, its function can be measured better near the wrist. Since the fingers and thumb-controlling muscles are closer to the skin

Table 2.1: The wrist and finger controlling muscles

	Superficial		Deep	
	Muscle	*Action*	*Muscle*	*Action*
Wrist Controlling	Flexor Carpi Radialis (FCR)	wrist flexion and abduction	The wrist control does not have any deep muscles	
	Palmaris Longus (PL)	flexion of wrist		
	Flexor Carpi Ulnaris (FCU)	flexion and adduction of the wrist		
	Extensor Carpi Radialis Longues (ECRL)	extension and abduction of the wrist		
	Extensor Carpi Radialis Brevis (ECRB)	extension and abduction of the wrist		
	Extensor Carpi Ulnaris (ECU)	extension and adduction of the wrist		
Finger Controlling	Flexor Digitorum Superficial (FDS)	flexing PIP joints	Flexor Digitorum Profundus (FDP)	flexing Distal phalanges
	Extensor Digitorum Communis (EDC)	extending fingers at MCP and interphalangeals joints	Flexor Pollicis Longus (FPL)	flexing the thumb
	Extensor Digiti Minimi (EDM)	extending the little finger at MCP and interphalangeals joints	Abductor Pollicis Longus (APL)	abducting and extending thumb at CMC joint
			Extensor Pollicis Brevis (EPB)	extending thumb at CMC joint
			Extensor Pollicis Longus (EPL)	extending MCP and interphalangeal joints
			Extensor Indicis Proprius (EIP)	Extending index finger

surface near the wrist, this location was selected to collect biosignals for predicting finger movements.

2.2 Related works

2.2.1 Biosignals for prosthesis control

To improve the performance of the partial hand prosthesis, researchers have investigated different non-invasive signals for continuous finger movement estimation. These signal include Ultrasound Imaging, Optical Myography, surface Electromyography, and Force Myography.

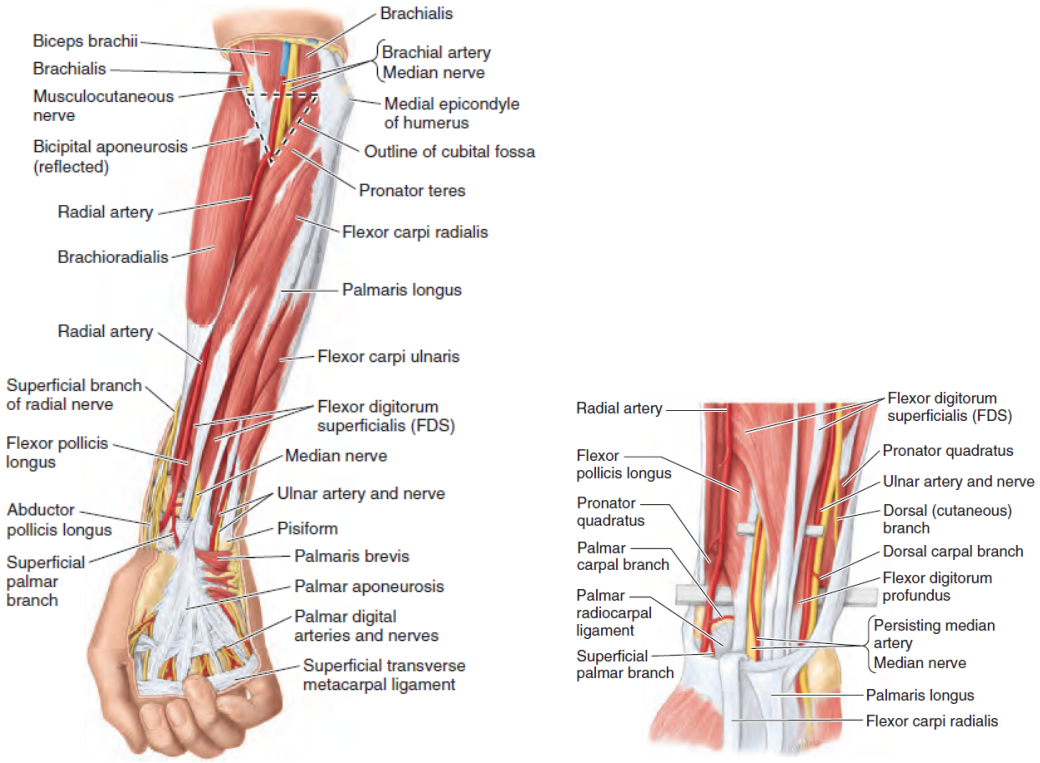

(a) (b)

Figure 2.2: Forearm and wrist muscles [17]

Ultrasound Imaging

Ultrasound (US) imaging is a non-invasive and common tool for diagnostic purposes. Since the US imaging is accurate, safe, and available in most hospitals, it is a good candidate for human-computer interface, and it can be potentially used for prosthesis control.

Castellini et al. [18] used US imaging to predict the angle of the MCP joints of the fingers and adduction and abduction of the thumb. They showed a linear relationship between spacial first order features extracted from the US images and the finger movements. Using a linear regression, they were able to achieve a Normalized Root Mean Square Error (NRMSE) value of 1.86% on average. They also implemented a motion compensation method to reduce the effect of the participant's small movements. However, extreme movements of the participant or transducer would defect the signal and had a negative effect on the performance.

In another study Sierra González and Castellini [19] estimated the continuous force applied by the fingers and thumb, using US imaging. They showed there is a linear relationship between the applied force and the features extracted from the US images. The authors used the maximum and minimum force that the fingers can apply for training their algorithm. While testing the algorithm, the range of the force that the fingers can apply was used. The results showed that it is possible to predict the continuous finger force with an NRMSE less than 10%. They also tested the system in an online setup and were able to get an NRMSE less or equal to 10% for all the fingers.

Sikdar et al. [20] used US imaging to classify the movement of each finger. They were able to achieve a classification accuracy of more than 95% using able-bodied participants. The authors also showed there is a correlation between the speed of the digits and the changes in the echogenicity of the US. The echogenicity of the tissue refers to the tissue's ability to bounce back US signal. The differences in the echogenicity of different tissues make the US image look black, gray or white, with white meaning the highest echogenicity and black means the lowest [21]. The correlation between the speed of the digits and echogenicity of the US image shows the possibility of using US imaging for estimating the speed of the digit movements.

In addition to using US imaging for continuous estimation of finger movements and force, several researchers have used this imaging method for hand gesture classification [22, 23, 24]. Although using US images as a control strategy has shown a good classification accuracy, its use as a portable device has limitations. The movement of the US probe can have a negative effect on the performance, and the probe needs to be connected to an on-site computer. These limitations would restrict its application as a real-time control strategy for externally-powered prostheses.

Optical Myography

Optical Myography (OMG) is a relatively new biosignal. OMG uses a camera to track changes caused by muscle movements on the skin surface.

Nissler et al. [25] used a standard webcam along with visual feedback markers on the participant's forearm to predict the continuous movements of the fingers. They trained the

system on the data collected during full flexion and rest state of the finger and tested it on the participant's range of motion. They were able to predict finger movements with an NRMSE of 0.13 to 0.2. Their work indicated the possibility of using OMG to estimate continuous finger movements.

In another study, Wu et al. [26] used colored tape and yarn pieces to mark the participant's forearm. They used a camera to track the changes on the participant's forearm due to different hand gestures. Wu et al. [26] indicated that there is a relationship between hand gestures and the optical map of the participant's forearm.

The OMG signal is a new signal and has practical limitations. As the studies that were done so far show, to collect a reliable signal, markers should be used on the participant's forearm. The use of the camera can cause problems regarding the portability of the system. In addition, the camera-based system is sensitive to lighting and occlusion, which can have an adverse effect on the system's performance.

surface Electromyography

Surface Electromyography (sEMG) is the most common biosignal to control prosthesis hands and partial hand prostheses. sEMG measures the electrical activity of the muscles and has been studied by several researchers to provide continuous control of the prosthesis hand for amputees.

Smith et al. [27] used sEMG to estimate the angle of MCP joints of fingers and thumb, while the wrist and elbow are in a fixed position. They used the artificial neural network as their regression model and were able to achieve an overall average correlation of determination (R^2) of 0.7423. They also show that the average R^2 value improves for each angle during the segment of the time series that the finger is the primary mover. The R^2 value, in this case, is 0.8468 on average. As a result, they suggest that performing a classification before the regression to identify the primary moving finger can improve prediction results.

Ngeo et al. [28] utilized sEMG along with Neural Network regression to predict the MCP, PIP and the DIP joints of fingers and thumb, which creates 14 angles in total. Running the experiment on one able-bodied subject, they were able to reach an R^2 value as high as 0.92 for Index finger's MCP joint. They took one step further and combined random finger

movement with their test data. A 5-fold cross validation analysis resulted in above 0.8 R^2 value for MCP joints, while PIP and DIP did not perform as well.

Pan et al. [29] predicted PIP and MCP finger joint angles while they keep the subject's upper limb in a fixed position using sEMG signal and state-space model. They were able to get an average of 0.824 R^2 predicting the angles of thumb, index, middle and ring fingers.

Although the studies mentioned above were able to achieve a high R^2 value, none of the experiment setups included variations regarding wrist and elbow angle.

As a result, in a follow-up work, Pan et al. [30], conducted data in different wrist positions from the middle finger of 6 able-bodied participants and index finger of 2 partial-hand amputees. They also adopted a two-step machine learning algorithm, where first a linear classifier identifies the wrist position, and then a suitable regression model is applied to the data to predict the joint angle value. They were able to get an R^2 value of about 0.8 on average, which proves the feasibility of using sEMG signal to predict fingers' continuous movements in the presence of wrist positions variations.

Although the sEMG signal has been extensively studied by researchers [27, 28, 29, 30], it has some disadvantages that can limit its practicality. To record the sEMG signal, skin preparation is necessary; the signal is sensitive to the users sweating; also, electrical noise has a negative effect on the sEMG signal [31]. In short, the sEMG signal is unstable due to environmental factors and user-based factors, such as sweating. These disadvantages resulted in marginal progress despite extensive research on the signal [32].

Force Myography

FMG is defined as tracking the volumetric changes in a muscle associated with the muscles contraction or relaxation during the functional movement of the limb [33]. Since in this work FMG was used as the myosignal, this signal will be explained in more details.

FMG is also known as residual kinetic imaging (RKI) [34]. The usage of the FMG signal has become more popular in the past decay. Phillips and Craelius [34] used a silicon sleeve to track the changes in the forearm shape, corresponding to different finger movements with two transradial amputee participants. The sleeve tracked the changes of the residual limb, using air cushions. The air cushions were used to track the changes in the residual limb

when the participants attempt to move their missing fingers. Their result indicates that, as the participants attempt to move different fingers, the movement of the muscles produce different patterns on the sleeve. They conclude that the FMG pattern on the residual limb can be used to determine which finger the participant is trying to move.

In a complementary research Phillips [35], tested air cushions and force sensing resistor (FSR) to classify hand gestures and movements. FSRs are polymer thick film (PTF) devices that show a decrease in resistance by increasing the applied force on their surface. The results suggested that, since the air cushions are fragile and likely to leak, FSRs have an advantage over them, and are a better sensor to record FMG.

Wininger et al. [33] used an array of 14 FSRs on the participant's forearm to predict the grip force applied by the participant continuously. Nine healthy subjects participated in their experiment. After analyzing the FMG data, the authors were able to achieve a mean cross-correlation of 0.89 between the FMG signal and applied grip force. The result indicated the signal's potential to estimate the grip force continuously.

Since then, several researchers have investigated the FMG signal's performance for hand gestures, finger movement, and wrist movement classification, in both amputee and non-amputee individuals [36, 37, 38, 39]. In addition to that, the performance of the signal for estimation of the force applied by the fingers and applied force and torque of the wrist have been investigated [40, 41, 42].

Regarding the classification Cho et al. [38], used FMG signal collected from the residual and intact limb of four transradial amputees to classify 6-11 different hand gestures. They compare the classification accuracy between the signal collected from the residual limb and the intact limb. Their investigation indicates that the residual limb has a lower accuracy during the classification, due to the degraded muscle tone. However, they were able to classify six hand gestures with a good accuracy in the residual limb. Further investigation revealed that when they subdivided the grips into the opposed thumb and non-opposed thumb modes, they were able to improve the accuracy further. Although the classification result looked promising, the signal variations with different elbow angles had not been considered in this study, and the elbow was kept in a fixed position.

Fougner et al. [43] demonstrated that when the classification system, using sEMG signal, is trained based on the data collected in a specific static position, for example keeping the elbow angle in 90°, it will not perform well during testing in different limb positions. The same problem exists for the hand gesture classification using FMG signal [44].

To overcome the aforementioned challenge Radmand et al. [44] introduced a high-density FMG. They were able to classify hand and wrist motions with a low classification error. They suggested to include data from eight different static positions in the training dataset. These positions were defined as specific locations in 3D space in front of the participant to cover a person's workspace and ensure proper performance with limb position variation. Their work resulted in classifying hand and wrist gestures in 3D space with a high classification accuracy.

Considering the continuous prediction, Castellini and Ravindra [40] used a cuff which was equipped with 10 FSRs, on the forearm of ten able-bodied subjects, to estimate the force applied by each finger and the rotation of thumb on a force sensor. They were able to estimate the force with about 1.5N error, while the force inserted by the fingers is in the range of 0 - 15N.

As FMG signal demonstrates promising results for hand and wrist classification, Kadkhodayan et al. [45] used the signal for continuous finger movement prediction to develop a prediction strategy for continuous finger movement. In a static setup, Kadkhodayan et al. [45] recorded the relative displacement of the tip of the index and middle finger and thumb with respect to a reference point on the hand, during tree hand movements. The result of ten-fold cross-validation using an epsilon support vector regression indicates an average R^2 of 0.96.

During the data collection, Kadkhodayan et al. [45] asked the participants to keep their wrist and elbow in a fixed position. In partial hand amputees with an intact and functional wrist, the finger movement is accompanied with wrist movement which can have a negative effect on the system's performance [30]. Different wrist positions are considered in the present study. The FMG signal is analyzed to determine whether the same effect of the different wrist positioning in sEMG can be observed in FMG signal or not.

Among the researches that so far covered FMG signal, three machine learning algorithms were more common, namely Linear classification and regression, Support Vector algorithm, and Neural Network algorithm. To cover **objective 1**, these three conventional algorithms will be tested on the FMG signal. In addition to the conventional algorithms Random Forest is suggested to be used by the author. It will be explained in the chapter 3 in more details that why this new algorithm can be a good alternative to the commonly used algorithms.

2.2.2 Wrist location variation and the effect on the signal

In designing of partial hand prosthesis for individuals with a functional wrist, it is essential to consider both accurate performance and the individual's ability to use their wrist [14]. It was mentioned earlier that the forearm and wrist include muscles that are responsible for both finger movement and wrist movement.

Adewuyi et al. [5] trained a pattern recognition system using sEMG on neutral wrist position to classify three hand gestures, and tested it in different wrist positions. In the case of training and testing on the neutral wrist position, they were able to achieve a classification error about 3%. When they tested the same system on different static wrist positions, the error increased to 12%. The authors also trained the system with the data collected in different wrist positions and tested it on different wrist position, and the error rate was decreased to about 4%. Their work indicated the effect of the wrist position variation on the system performance, and the necessity of including different wrist positions in the training phase.

In a follow-up work Adewuyi et al. [14] included partial hand amputees in their study and used four hand gestures. In agreement with their previous work, their work supported the importance to train on different wrist positions rather than just one wrist position. The authors also mention that it is important to reduce the number of wrist positions during the training to avoid fatigue for the user.

In addition to these works Pan et al. [30] trained their system on different static wrist positions to compensate for wrist movement. To the best of our knowledge, the effect of wrist position variation on the FMG signal was not investigated before, and it will be considered in the present work.

2.3 Summary

Different non-invasive myosignals for predicting continuous finger movement were explained in this chapter. These myosignals include US, OMG, sEMG, and FMG.

One of the limitations of US and OMG signals as real-time and portable control strategies is that they need sizable equipment to be recorded precisely. The US imaging technique needs a probe that should be connected to a computer for data collection. The probe needs to be placed with specific consideration to be able to record muscle movements and functions. The US probe may move during the use, and the movement can have a negative effect on the signal. These limitations can affect its performance as a prosthesis control strategy.

When recording OMG signal, as it is a camera-based signal, it is sensitive to lightning, and occlusions may distort the image. The camera needs to be placed precisely to have the forearm in the field of view. In addition, researchers so far have been using markers on the skin to determine the movement of the muscles. The limitations mentioned above can prevent the use of the system as a prosthesis controlling technology.

sEMG technique is the most frequently used technique for controlling prosthesis devices, due to its non-invasiveness and demonstrated ability for hand classification. However, this technique can pose some disadvantages such as sensitivity to electrical noise and users' sweating [31].

As a result, FMG has been investigated as a cost-effective alternative to sEMG. The FMG technique can overcome the difficulties regarding the user and the environment. The electrode placement for FMG signal collection does not need any skin preparation, and the signal is not sensitive to sweating or electrical noise.

Toward providing a control strategy, in addition to the biosignal selection, the effect of the wrist movements on the biosignal should be considered.

In the end, the advantages of FMG signal has motivated us to investigate its ability to provide a proportional control for partial hand prostheses. Moreover, the importance of wrist movement motivated us to investigate its effect on the FMG signal performance during grasping movement estimation.

To the best of author's knowledge and as presented in this chapter, previous researches on FMG signal did not include continuous finger movements in different wrist position. Since sEMG is a more established signal, there are studies which consider wrist positions with sEMG signal. These studies suggest that there is a need to do a classification first to identify the wrist position and define different models for different wrist positions. In chapter 5 the same approach is tested on the FMG signal, as well as an approach suggested by the author. The comparison between the two approaches help to identify the proper approach toward the goal of this study.

Chapter 3

Machine Learning Algorithms

In this chapter, an overview of different machine learning algorithms that have been previously used in the literature on the FMG signal for classification and regression are explained. Also, Random Forest is introduced as a non-conventional machine learning algorithm. The presented information in this chapter can help to cover **objective 1**. In the examples and explanations, the target value for the algorithm is denoted as Y, the sample points are denoted as x, and the number of sample points is N. Each sample points consists of M features. The feature vectors are denoted as $f_1, f_2, ..., f_M$. The features included in the sample point x_i are noted as $f_{i1}, f_{i2}, ..., f_{iM}$.

3.1 Linear classification and regression

The linear regression and classification have been used on FMG data for continuous finger force prediction and hand gesture classification [31, 33, 38, 40]. A linear combination of the features is used to create the linear regression model.

$$Y = \sum_{i=1}^{M} \alpha_i f_i + \alpha_0 \tag{3.1}$$

In the Formula 3.1 α_i is the weight of each feature in the model and f_i denotes each feature. M indicates the number of features. In the case of the regression, the output of the model is a continuous variable. Figure 3.1 illustrates an example of the linear regression method.

For multi-class classification, a Y value is defined for each class:

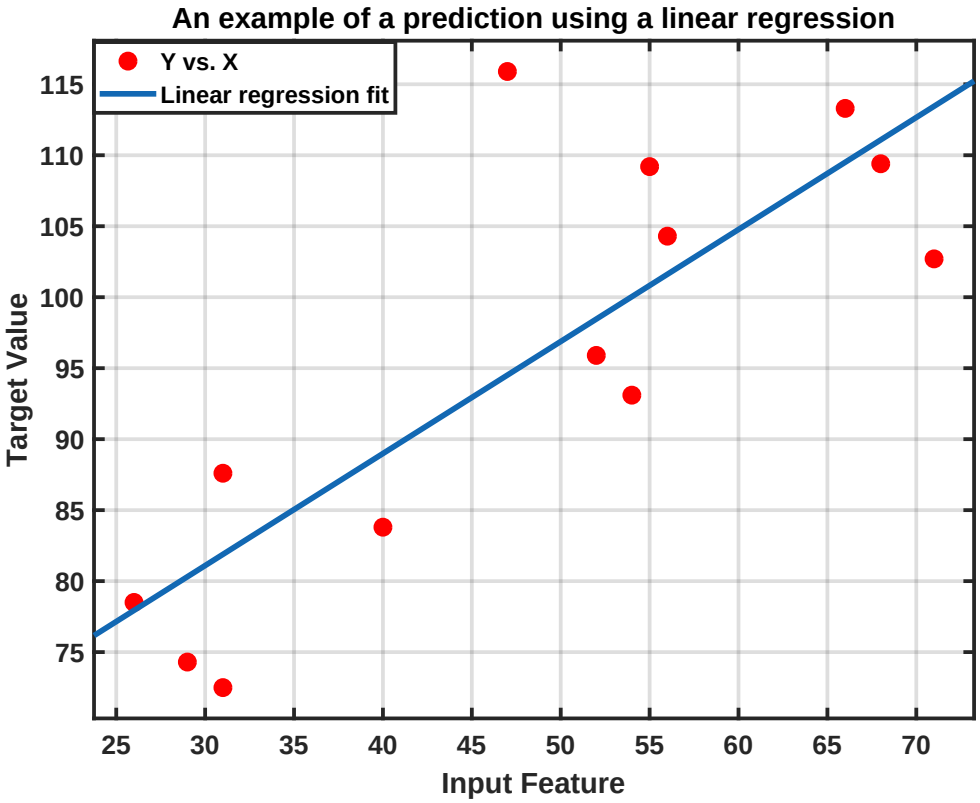

Figure 3.1: The example of the performance of the linear regression

$$Y_k = \sum_{i=1}^{M} \alpha_{ik} f_i \tag{3.2}$$

In the formula 3.2 k indicates the index of the class. For a K-class problem we have $k \in 1, .., K$. To determine the class that a new point belongs to, the Y_k for each class is calculated, the point belongs to class k, if $Y_k > Y_j$ for all $j \neq k$ [46]. Figure 3.2 shows an example of a linear classifier. The *fisheriris* dataset in MATLAB 2017b is used as the data set to illustrate the performance.

Linear regression and classification are computationally efficient [31]. They can perform well, where the target value has a linear relationship to the presented features, or in a classification case, the two classes are linearly separable. Although in some cases a linear relationship cannot be established between the features and targeted value. In those cases, other algorithms can be used.

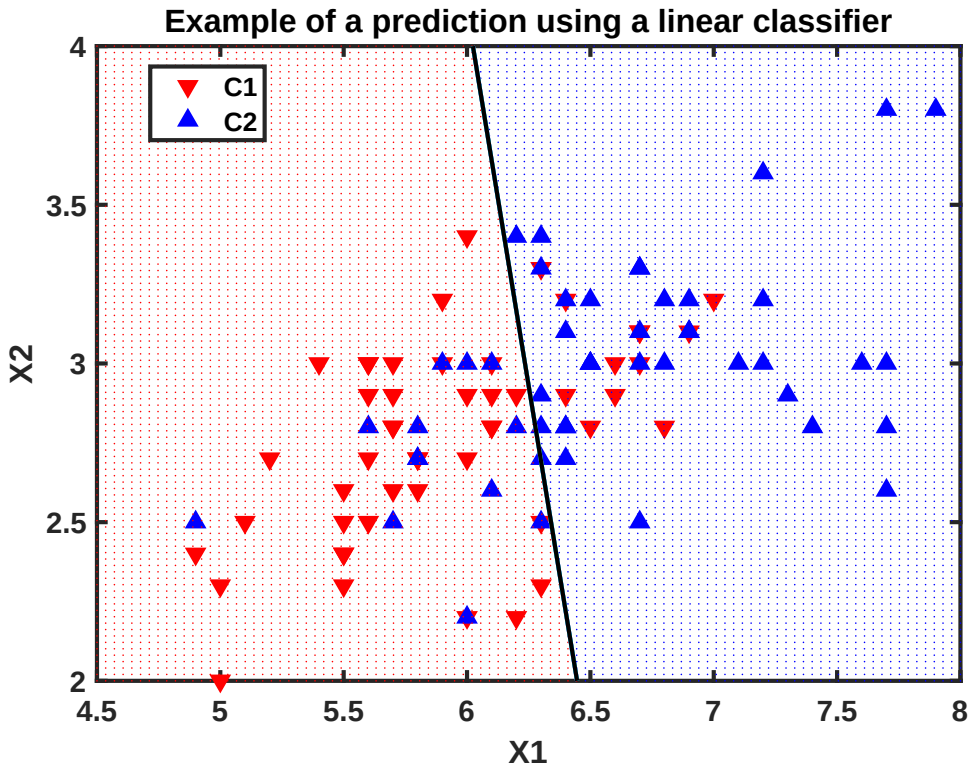

Figure 3.2: The example of the performance of the linear Classifier

3.2 Support vector machine

In addition to linear regression and classification, the Support Vector Machine (SVM) algorithm has been used in the literature for classification and regression [45, 41, 47].

In SVM classification, similar to the linear classification, the algorithm is trying to find a line (in a two dimension problem), or hyperplane that separates the classes from each other. In a linear classification, all the training data points are involved in finding the separation line. In contrast, in an SVM classifier, only a subset of data is involved in finding this line. The subset data, are the data points that lie in a defined *margin*. The margin is defined to be "the smallest distance between the decision boundary and any of the samples" [46]. The points in the margin that are used to determine the boundaries are called Support Vectors (SVs).

In addition to the SVs, the SVM algorithm uses *Kernel trick*. By using Kernel functions, the input data are transformed to the kernel function's space, to find a linear relationship

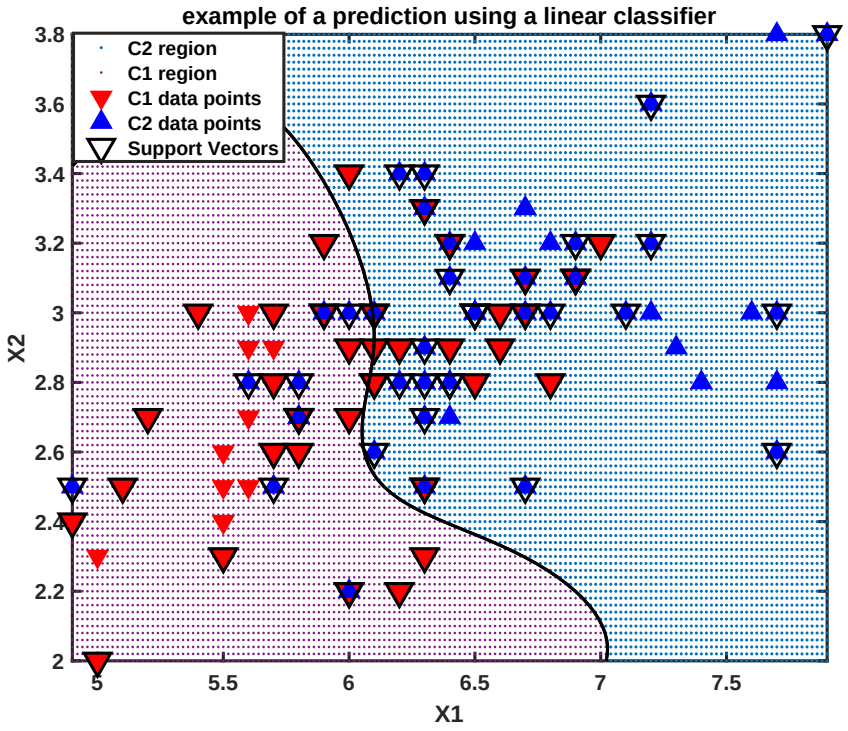

Figure 3.3: The example of the performance of the SVM Classifier

between the input value and the target value. Different functions can be used as the kernel function. One of the kernel functions that is commonly used is the Gaussian kernel.

$$K(f_i, f_j) = e^{-\frac{\|f_i - f_j\|^2}{2\sigma^2}} \tag{3.3}$$

Formula 3.3 indicates the calculation of the Gaussian kernel. f_i and f_j are different feature vectors, σ is the Gaussian kernel parameter and needs to be determined by the user. After applying the kernel function on the input, instead of using f_i and f_j for training $K(f_i, f_j)$ will be used for training. As a result, the relationship between the target and sample points will be:

$$Y \approx K(x) \Rightarrow Y \approx K(f_1, f_2, ..., f_M) \tag{3.4}$$

Figure 3.3 indicates the performance of a SVM classifier. The data is the same as the data used in Figure 3.2. The black line indicates the separation boundary. The points marked with black triangle indicate the points as the Support Vectors.

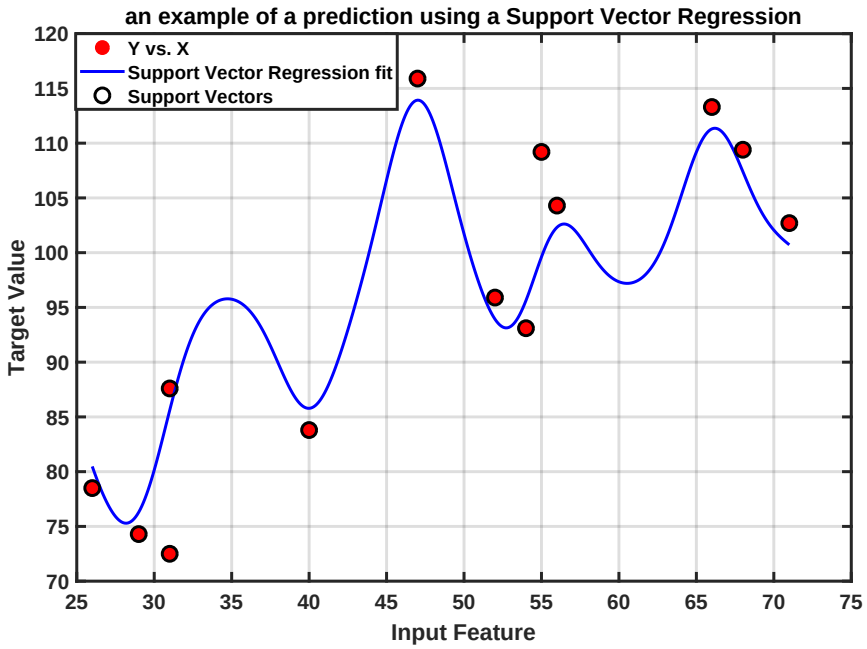

Figure 3.4: The example of the performance of the Support Vector regression

For regression, the same approach is used. The support vectors in the case of a regression, are contributing to the creation of the model. Figure 3.4 illustrates an example of the Support Vector Regression (SVR). The data used is the same as Figure 3.1. Since the number of data points is small, all of them have been used as support vectors to estimate the curve. It can be seen in the figure that the curve is over-fitting. Using the SVR algorithm on a small dataset would cause over-fitting, which can reduce the accuracy of the performance on a new dataset.

The SVM algorithm can be a proper approach to predict the non-linear relationship, as it can use different kernels on the input data. In addition, since it uses the support vectors, and not the whole data set, the effect of the outlier data will be minimized. While using the SVM algorithm, one should keep in mind some considerations. The SVM algorithm can be computationally expensive and time-consuming, as the user needs to optimize the value of the hyperparameters, which may require multiple running. SVM is also extremely sensitive to the selection of the kernel function and its hyperparameters [48]. The parameters should be selected carefully to ensure good performance from the algorithm.

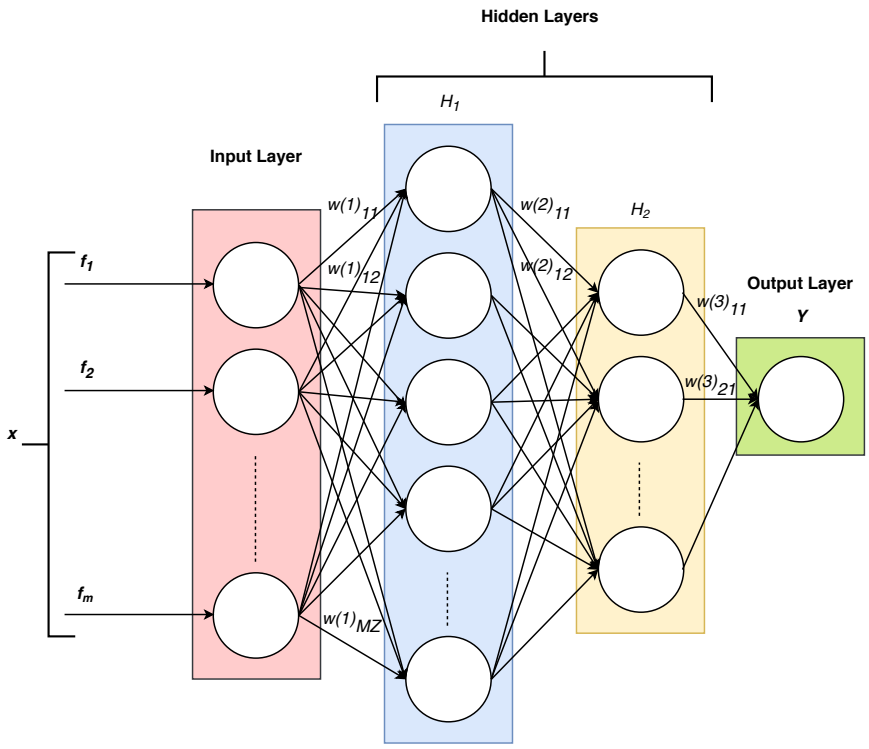

Figure 3.5: An example of a Neural Network structure

3.3 Neural network

Another regression method that has been used in the literature for estimating continuous force from FMG signal is Neural Networks regression (NNR) [42]. A Neural Network consists of an input layer, an output layer, and some hidden layers. Figure 3.5 indicates an example of a Neural Network (NN) structure. Each layer of the NN consists of several nodes. The nodes of the input layer are the features constructing each sample. All the features can be used as the input for the network. The output of each layer will be multiplied by a weight value and used as the input for the next layer. Each layer has a specific activation function, that gets the input and produces the output of that specific layer. The output layer calculates the target value. Figure 3.6 shows an example of a neural network regression. The estimated curve does not have high accuracy, as the training set only includes 13 points.

Another simple example of the Neural Network performance is as follows:

$$
\begin{aligned}
&H_1(z) = z \\
&H_2(z) = e^{\frac{-z^2}{2}} \\
&H_1(x) = f_1 \times w_{11}^{(1)} + f_1 \times w_{12}^{(1)} + ... + f_m \times w_{MZ}^{(1)} = W^{(1)}.x \\
&S = W^{(2)}.H_1(x) \\
&H_2(S) = e^{\frac{-S^2}{2}} \\
&Y = W^{(3)}.H_2(S) \\
&Y = W^{(3)}.e^{\frac{-(W^{(2)}.(W^{(1)}.x))^2}{2}}
\end{aligned}
\tag{3.5}
$$

The NN in Formula 3.5 has 2 hidden layers. Each layer has an activation function. The first layer uses a Linear function, and the second layer uses an exponential function as the activation function. Layers can have a variety of activation functions. The output layer can get an activation function as well. In the presented example the output layer is a linear function. Formula 3.5 shows how the NN calculates the output for a data point.

The number of nodes in each layer and the number of layers need to be optimized, in training an NN. In addition, the activation function of each layer can need a parameter optimization. For example, if a Gaussian function is used as an activation function in a layer, the value of "σ" needs to be optimized and chosen carefully.

The neural network can perform well when the relationship between features and the target value is non-linear, and it may need a notable amount of input data, depending on the number of the weights it needs to find. Similar to SVM, NN has different parameters to optimize (number of nodes, number of layers, hidden layers' hyperparameters), which is computationally expensive, and time-consuming [1].

3.4 Random Forest

Random forest (RF) algorithm has potential advantages over conventional machine learning algorithms. Some of the advantages are as follows. The RF algorithm is robust to overfitting;

[1] https://www.cs.cmu.edu/ schneide/tut5/node28.html#tabcomparison

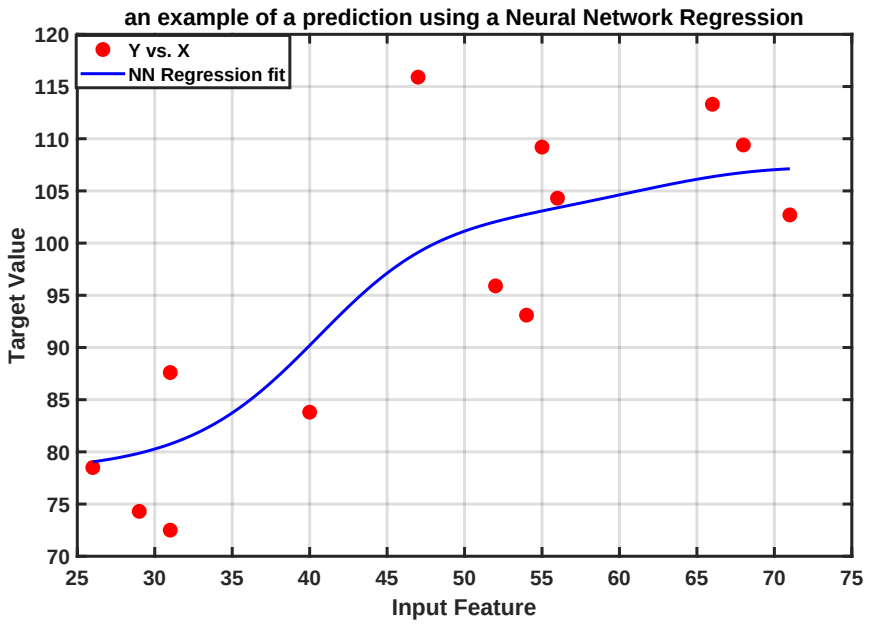

Figure 3.6: The example of the performance of the Neural Network regression

it has only two parameters to optimize (the number of variables in the random subset at each node to split and the number of trees in the forest), while it is not very sensitive to these parameters [49, 50]. The advantages of the RF algorithm can make it a potential alternative to the conventional algorithms, for the goal of this study.

Random Forest is an ensemble of un-pruned trees. Consider a dataset that has N data points, and each data point is constructed from M features. In the random forest algorithm developed by Breiman [49], to construct each tree a random subset of the samples including N' data points is selected. In a standard tree each node is split based on all M features, but in the algorithm developed by Breiman [49], each node is divided using the best guess among a random subset of the features. So instead of using all M feature to make a decision at each node, M' features are used to make a decision. The prediction of a new sample is made by aggregating (the majority of votes for classification and averaging for regression) the prediction of the whole forest.

For example, consider the two-class problem presented earlier. Both linear classifier and SVM classifiers were using the data to define a separation boundary. In the Random forest algorithm, the data is used to define different sub-regions for each class. Figure 3.7 illustrates the regions defined using the RF. The RF model is a forest of trees constructed from the

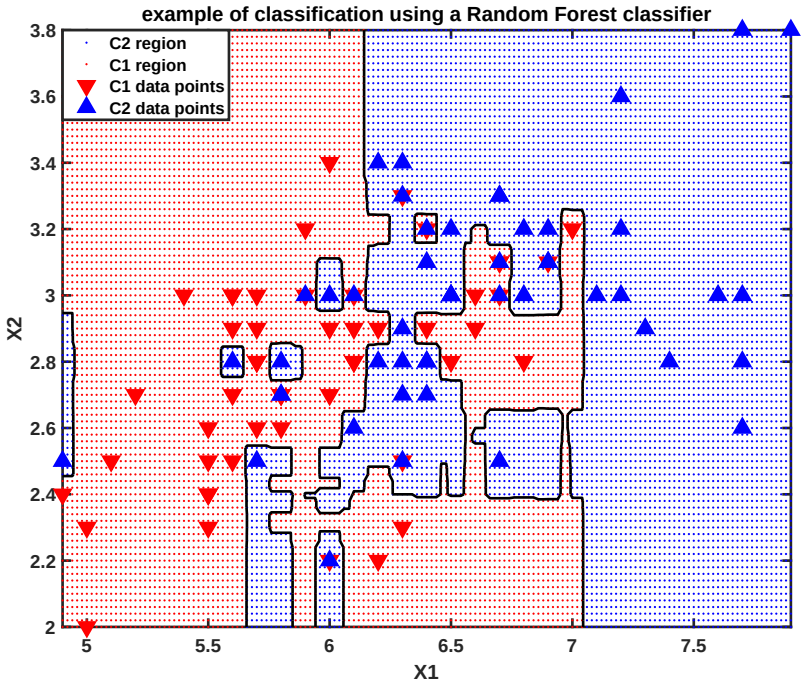

Figure 3.7: An example of the Random Forest performance

features to classify the data. The RF model in this example consists of 100 tresses. To classify a new data point, the features of the data point will follow the tree structures to find the proper class. This will be done for all trees, and the majority of votes will determine the class of the point.

To solve a continuous problem the same approach is used for regression. To solve the regression problem for a new data point the features will follow the trees. The average result of all the trees shows the result corresponding to the data point. Figure 3.8 illustrates an example of the performance of the random forest regression. It is important to keep in mind that the number of features provided and the number of the data points are small, as a result, the performance may not be good. Figure 3.9 indicates nine of the trees used for the regression. As an example consider we want to get the output value for the input of $X = 45.5$, using a model including only the trees illustrated in Figure 3.9. The point will go through the trees in Figure 3.9 a-i, and it will result in 77.9, 85.07143, 81.7125, 105.125, 76.94286, 83.81429, 93.68333, 99.3625, and 98.6625. The forest results in 89.1416 on average, which would be the final result of the prediction.

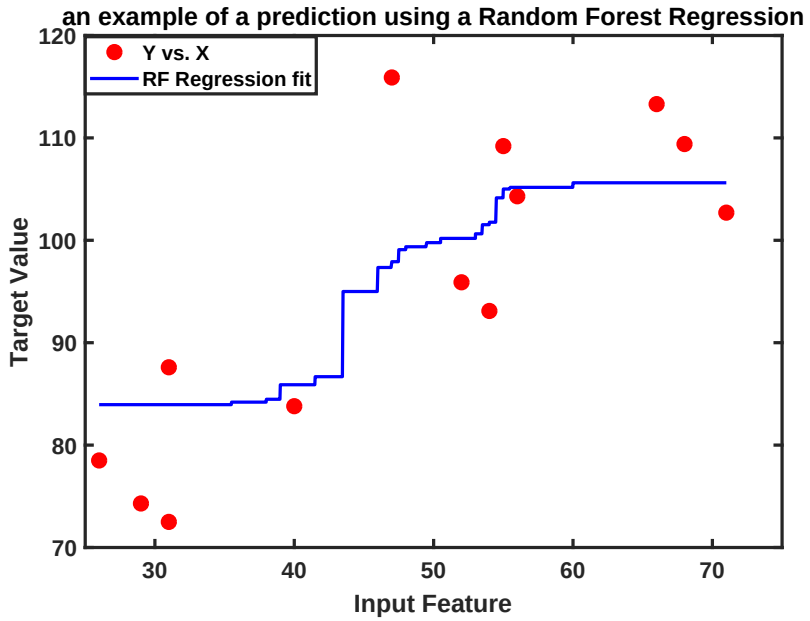

Figure 3.8: The example of the performance of the Random Forest regression

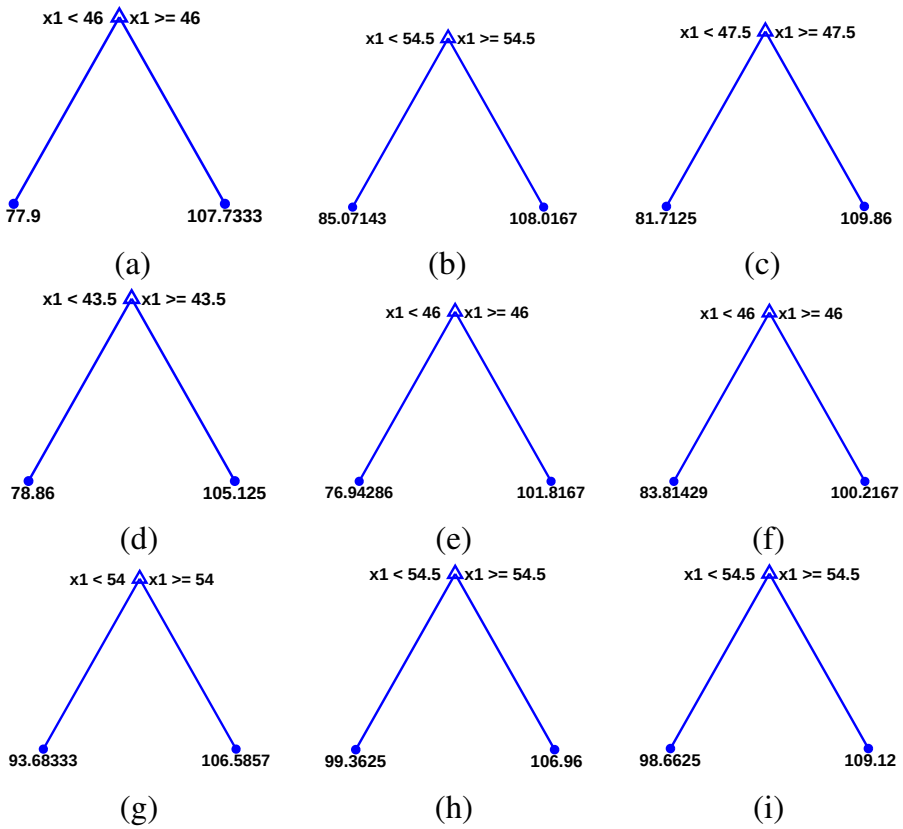

Figure 3.9: Nine trees of the Random Forest model

In this research, the random forest package of Matlab (introduced in R2009a) was used. The number of trees was set to 100. Matlab's default was used for the number of random features to use for splitting at each node (M'), which was the square root of the number of features for classification ($M' = \sqrt{M}$) and one-third of the number of features for regression ($M' = \frac{M}{3}$). Matlab's default was also used to determine the size of the random subset of the data (N') to construct each tree, which was the same as the size of the training dataset ($N' = N$). In our case, we have 18 sensors which provided 18 channels; thus four random features were used for classification and six random features were used for splitting at each node for regression.

3.5 Summary

Different machine learning methods have been used for classification and regression, using the FMG signal. In this chapter three of the most common algorithms were explained. In addition to the three common machine learning algorithms, Random Forest is introduced and explained, as a non-conventional machine learning algorithm for regression and classification using FMG signal. Each algorithm has its advantages and disadvantages. Based on the requirements, one would prefer one over the other.

Later on to cover **objective 1** all the mentioned machine learning algorithm will be used to regress and classify the FMG signal. As it was mentioned in chapter 2, the common approach to do finger and hand movement regression or classification in different wrist positions, is to use a classifier first to determine the wrist position that hand is in. To test the common approach for FMG data three classification methods, Linear Discriminate Analysis, Support Vector Machine, and Random Forest had been investigated and compared in the present work. In addition, four regression methods, Linear Regression, Support Vector Regression, Neural Network Regression, and Random Forest are explored and compared. The comparison between classifiers and regressors covers **objective 1**. The method and results of the comparison are covered in chapter 5.

The next chapter will cover the Experimental material and methods.

Chapter 4

Experimental Setup and Protocol

This chapter will provide insights into the used experimental protocol to collect the data to experiment the finger movement prediction using the FMG signal. The experimental protocol and setup were designed to include hand movement data from different wrist positions. In the following first an overview of setup and protocol is provided, which outlines the relationship between the objectives and the protocol and setup. In the second section, the hardware design is provided which includes the design of the FMG band data collection, and a custom-made brace to control the movement of the participant's wrist. Then the experimental protocol is explained in detail. After, the software that was used to collect synchronized data from the FMG data collection band and the motion capture system (true value of the finger movements) is explained. The selected grasp types and wrist positions, and processing of the hand motion data are explained subsequently.

4.1 Setup and protocol overview

Toward the goal of the project, the protocol was designed to collect data from different hand movements in different wrist positions. Each part of the setup and protocol will be explained in detail in the following sections. This section provides an overview of how the setup and protocol are designed to cover **objective 1** and **objective 2**.

The first step is recording the FMG data. It was explained in section 2.1 that the proper placement of the band is near the wrist as the changes of digit controlling muscles and tendons are more visible on that specific location. The circumference of the limb near the wrist is smaller compared to the forearm. The circumference was a motivation to use small

size sensors to have a higher resolution. The collected FMG data are used to explore different regression models and classification models (**objective 1**, part 1 and part 2). Moreover, the data is used to validate the use of signal and investigate the effect of the movement on the signal (**objective 1** part 3 and **objective 2**). To cover part 3 of **objective 1** and the **objective 2**, it is desired to eliminate unwanted movements and restrict the wrist to specific positions as the first step to validate the usage of FMG with different wrist positions and to investigate the effect of the wrist position. To do so, a brace was designed and made to keep the participant's wrist in each specific position. Section 4.2 includes detailed information about the FMG data collection band and the brace.

The next section explains the experimental protocol. The experimental protocol was designed to cover continuous hand movements in different wrist positions. **Objective 1** part 1, requires data from the continuous movement of the hand to use as the true value for regression. A motion capture system was used to track the 3D location of the fingers in the space. For recording the information of the wrist position, to use in a classification problem later, the position of the wrist was recorded for each data file. The name of each data file included the name of the position that wrist was in. The position information can specifically help to cover **objective 1**, part 2. Moreover, as the experiment includes different wrist positions, the analysis of the collected data can help to cover **objective 1** part 3, and **objective 2**

Section 4.4 describes the data collection software setup. The data collection software was setup based on the need to collect synchronized data from the motion capture system and the FMG band. A program in C# was coded to collect FMG data points and their corresponding 3D location data at the same time. The data is later analyzed to cover **both objectives**.

In the end, section 4.5 and section 4.6 explain the selection of the hand grasps and wrist positions as well as the selection of a measure of the hand movement.

4.2 Hardware design

As it was mentioned in section 2.2.1, different ways to measure the FMG signal have been investigated. Using FSR sensors to measure the FMG signal has shown to be a reliable way to measure the signal and they have been the most common sensors used to measure the FMG signal. Having this in mind, FSRs have been used in this research as well.

4.2.1 The FMG data collection band

Throughout literature different designs of the FMG data collection band has been used [13, 40, 51, 52]. All different designs include an array of Force Sensing Resistors. The number of sensors and the shape and placement of the band is different from one research to the other, based on the application and requirements. In this research as the small movements of the muscles and tendons near the wrist were of great interest, and to increase the resolution of the measurement, small FSR sensors were selected. An array of 18 Force Sensing Resistors (FSR® 400, Short, Interlink Electronics, Westlake Village, CA) were placed in a flexible band, cut from 2mm thick foam. FSRs are polymer thick film (PTF) devices that show a decrease in resistance by increasing the applied force on their surface. This specific model can be activated with 0.2N force, and its sensitivity range is up to 20N [53]. Figure 4.1.a shows a close view of a FSR. As the FSRs are flexible devices, by wrapping the band around the participant's wrist, each FSR will bend. To stop the FSRs from bending, each FSR was supported with a piece of 1.5mm thick acrylic sheet which was cut to the FSR's exact shape and dimensions. To concentrate the pressure from the wrist on the FSR's sensing area a piece of 1.5mm thick foam was placed on each FSR.

The sensors were placed on the flexible band 4mm apart from each other. Figure 4.1.b illustrates the FMG data collection band. As mentioned in the user guide [54] to have a force reading the sensor was connected to a resistor in a voltage divider circuit. The value of output voltage read from the resistor (VOUT in Figure 4.1.c) had been used as a representative of the applied pressure. The output voltage has shown to be acceptable to capture the FMG signal [55]. Figure 4.2 illustrates the circuitry of the band. An Arduino Pro Mini microprocessor was used to read the value of VOUT. The Arduino is powered by an ATmega

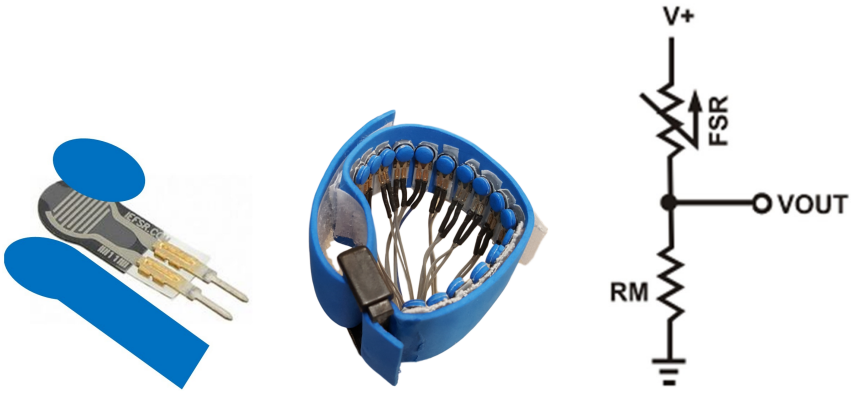

(a) (b) (c)

Figure 4.1: a. The configuration of hard backing and foam on the FSR b. The FMG data collection band c. The FSR circuitry. VOUT is recorded with the microprocessor

328. The D.C. power should be either 3.3V or 5V. In this work, the microprocessor was used with a 5V D.C. power. The Pro Mini board can connect to up to eight analog pins. To read the analog output from 18 FSRs in the band an analog multiplexer (Analog/Digital MUX Breakout - CD74HC4067, Texas Instruments, Dallas, TX) was used. The microprocessor was coded to read all the sensors every 0.066 seconds. The microprocessor was connected to an on-site computer with a USB cable, to record the data.

The band was placed on the upper limb above the head of Ulna bone. The buckle of the band was kept on the Radius bone. As it was explained in section 2.1 the reasoning behind this placement is that the muscles and tendons that control hand digits are mostly deep muscles. The nature of FMG is to pick up the effect of limb volume changes, from muscle and tendon movements, on the skin surface. On the forearm, moving from the elbow to the wrist, the digit controlling muscles get closer to the skin surface, and the changes would be more localized for the FMG band. It is worth mentioning that these changes are visible on forearm belly muscle as well, but they are more localized near the wrist. Since the changes regarding the digit movements were of great interest in this research this specific placement was selected.

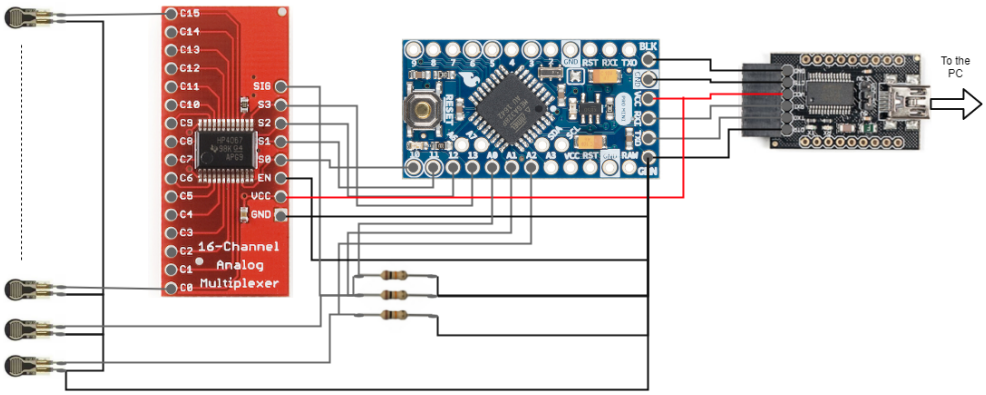

Figure 4.2: The circuit design of the band[1]

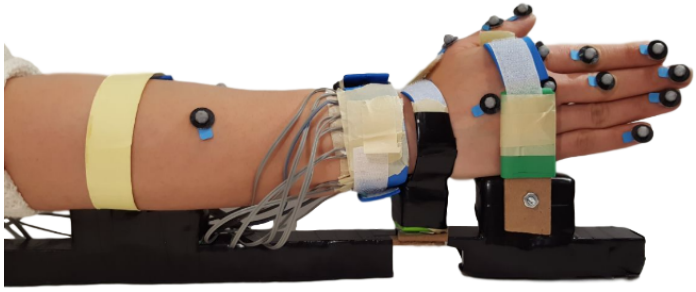

Figure 4.3: Participant's hand placement in the brace to eliminate undesirable movement

4.2.2 The brace

One of the goals of this study is to investigate the effect of the different static wrist positions. For this matter, it is essential to keep the positioning fixed, during collecting data for each wrist positions. To eliminate any other unwanted movement the participants' hand and forearm were fixed in a brace. Figure 4.3 illustrates the brace and hand placement in the brace. To maintain the participants' comfort pieces of the polystyrene foam were used as supports for forearm, wrist, and hand in the brace. The brace includes a joint under the wrist. For each wrist position, the nut and screw of the wrist joint were unlocked. Then the participant was asked to move their hand to the specific position. The nut and screw were locked after hand positioning.

[1]Photos of breakout boards: https://www.sparkfun.com; https://www.amazon.com

4.3 Experimental protocol

After designing the band to collect FMG signal and the brace to control the participants' wrist, the protocol was designed. Having the objectives in mind, the protocol was designed to include hand movements in different wrist positions. Toward the goal of the project different regression models for continuous hand movement need to be compared. As a result, the experiment included a precise motion capture system to track and store the finger movements data in real time. To be able to compare different classification models on the data, the data files from different wrist positions were labeled with the wrist position's name.

The band placement was kept uniform among the participants. It was placed on the upper limb above the head of Ulna bone. The buckle of the band was kept on the Radius bone. The participants sat behind a desk with an adjustable height. The height of the desk and their chair was adjusted in a way that participants could rest their elbow on the table. Their hand was placed in the brace. With this consideration, the elbow was kept at a relaxed angle and wrist was fixed at a specific angle during each data collection session. The data collection from each participant was performed in one session. Participants did not need to come back for follow up sessions.

To track the finger movements a motion capture system (Qualisys AB, Gothenburg, Sweden) was used. The system consists of eight cameras, fifteen markers, and the motion capture software which is called QTM. The cameras use short infrared flashes to illuminate the markers. QTM software was used to calibrate the system prior to the data collection with each participant. The qualisys 110 mm carbon calibration kit was used for calibration of the system (Figure 4.4). For calibration, the calibration set model, and the exact measurement of the calibration wand were entered in the QTM software. After selecting the calibration set, the 2D image of each camera was checked to make sure no external objects were adding noise to the cameras measurement. Cameras should be placed in a way that they do not see each other's face; otherwise, the infrared flashes from one camera can add noise to the other camera. Any reflective objects that could add noise to the cameras' image were removed

from the cameras' field of view. Then the desired field of view was swept with the calibration wand, while the calibration reference was placed on the data collection table.

The markers were placed on the participants' hand, wrist and forearm (Figure 4.5). On the index and middle finger, markers were placed on fingertips, PIP joint, and MCP joint. On the thumb, the markers were placed in the thumb's tip, IP joint, and MCP joint. On the wrist, the marker was placed on the Radiocarpal joint. On the forearm, the markers were placed on the Radius bone in line with the wrist marker and between Ulna and Radius perpendicular to the Radius's marker. Two markers were placed on the little and ring fingers' tip as well.

Each marker on the participant's hand should be visible to at least three cameras during data collection, for the QTM software to track the position of the marker in 3D space. Figure 4.6 shows the camera placement and the participant. Cameras were placed around the participant, to cover approximately 250° of the area around them. This placement will guarantee that all the markers are at least visible to three cameras, during data collection.

The data collected from the markers using the cameras were used to create a 3D model of the hand, digits, and forearm to track their movements. Figure 4.7 illustrates the 3D model constructed with the QTM software, using the motion capture data. The sampling frequency of the motion capture system was set to 100Hz. The sampling rate of the FMG band was set to 15Hz. This sampling frequency was sufficient to track finger movements in this study [45]. A minimum of 5Hz sampling frequency is necessary for the FMG data collection from the upper limb muscles [55].

4.4 Data Collection Software Setup

The QTM software can send real-time data on a TCP/IP protocol, on a local IP number [56]. The data packets include all the valuable information from the tracking system, for each frame, in addition to the frame numbers. The information from the tracking system is used as the true value of the movement. As a result, it is important to collect the FMG data and motion data in a synchronized manner. The TCP/IP connection protocol was used to collect synchronized data from the tracking system and the FMG band, to use in

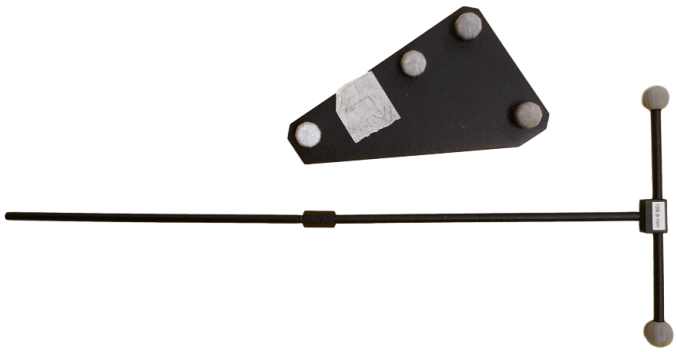

Figure 4.4: Carbon black,110mm calibration set for Qualisys tracking system

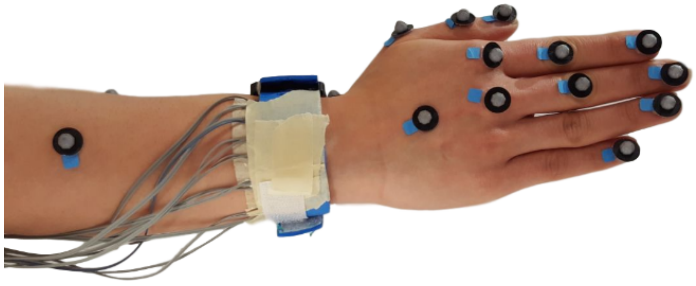

Figure 4.5: Band and marker placement on the participant's hand

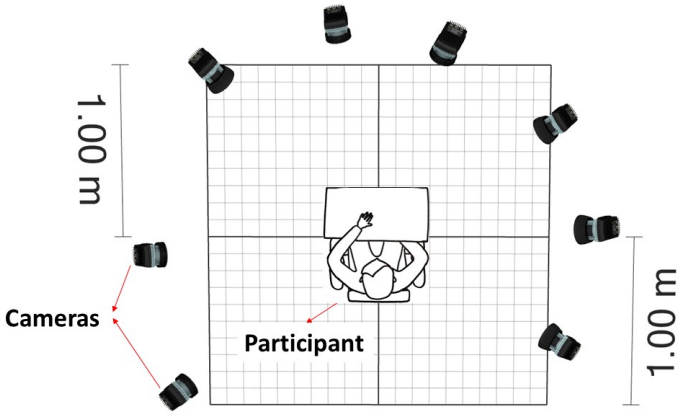

Figure 4.6: The camera placement around the subject

off-line processing. To collect data from the FMG band and the motion capture system at the same time a program in C# was coded. Figure 4.8 shows a simplified diagram of the data collection program. The program consisted of two threads. The threads are the

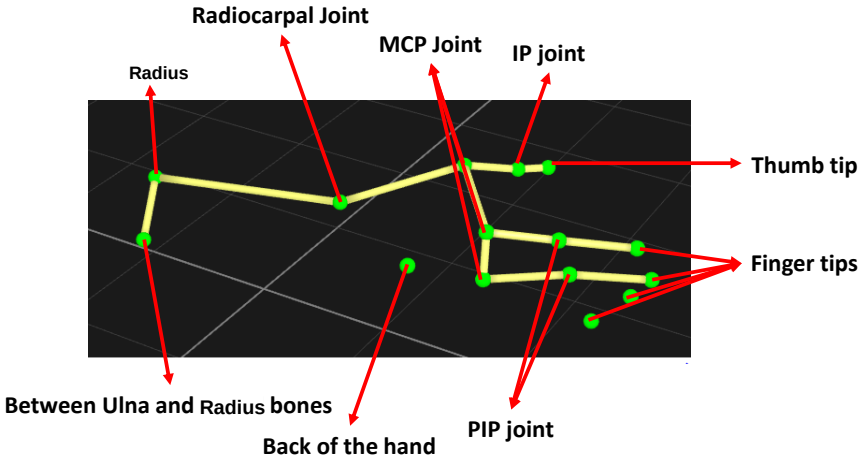

Figure 4.7: The constracted 3D model using motion capture data

main thread and the background thread. The TCP connection was monitored in the main thread, and the serial connection was monitored in the background thread. Whenever the background thread received a data point from the serial port, it read the corresponding TCP data packet from the main thread. From the desired data packet the frame number was extracted. The frame number and the serial port data are recorded and saved as a text file.

At the end of the data collection from each wrist position, the video from the motion capture system was saved and exported as a Matlab file using the QTM software. The exported file includes the complete information from the video, which included the 3D location of each marker in each frame as well as marker's name. This exported data along with the recorded frame number with the C# program were used to get the 3D location of the markers corresponding to each FMG band's data point. The frame number corresponding to each FMG data point was noted. The exported Matlab file was scan to find the desired frame numbers and the markers' location data of those frames were extracted.

4.5 Grasp Types and Wrist Positions

To investigate the effect of the continuous hand movements on the FMG three hand grasps were selected. In an attempt to estimate the continuous hand movement Kadkhodayan et al. [45] selected three grasp types, as a subcategory from Cutkosky's grasp taxonomy

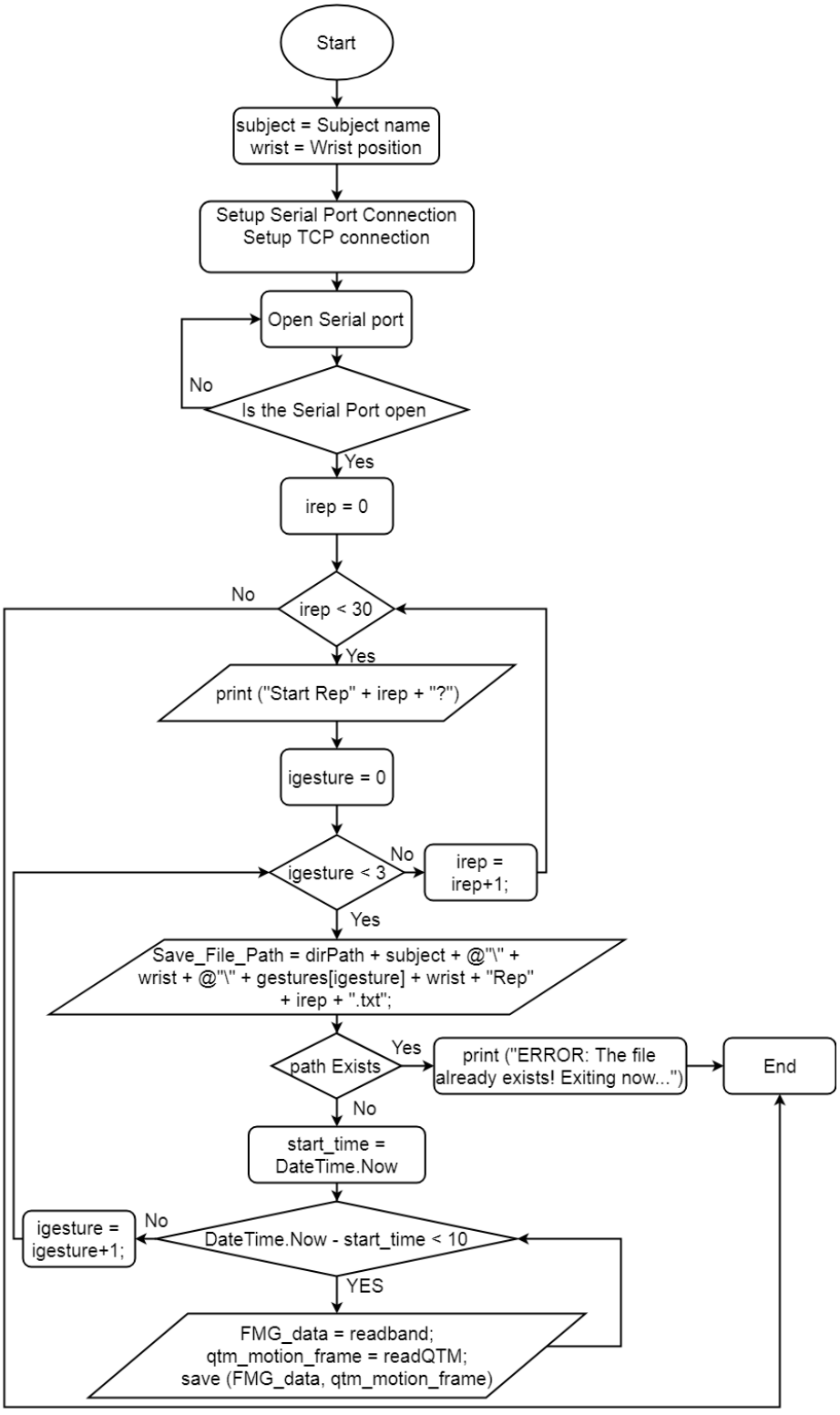

Figure 4.8: A simplified diagram of the data collection program

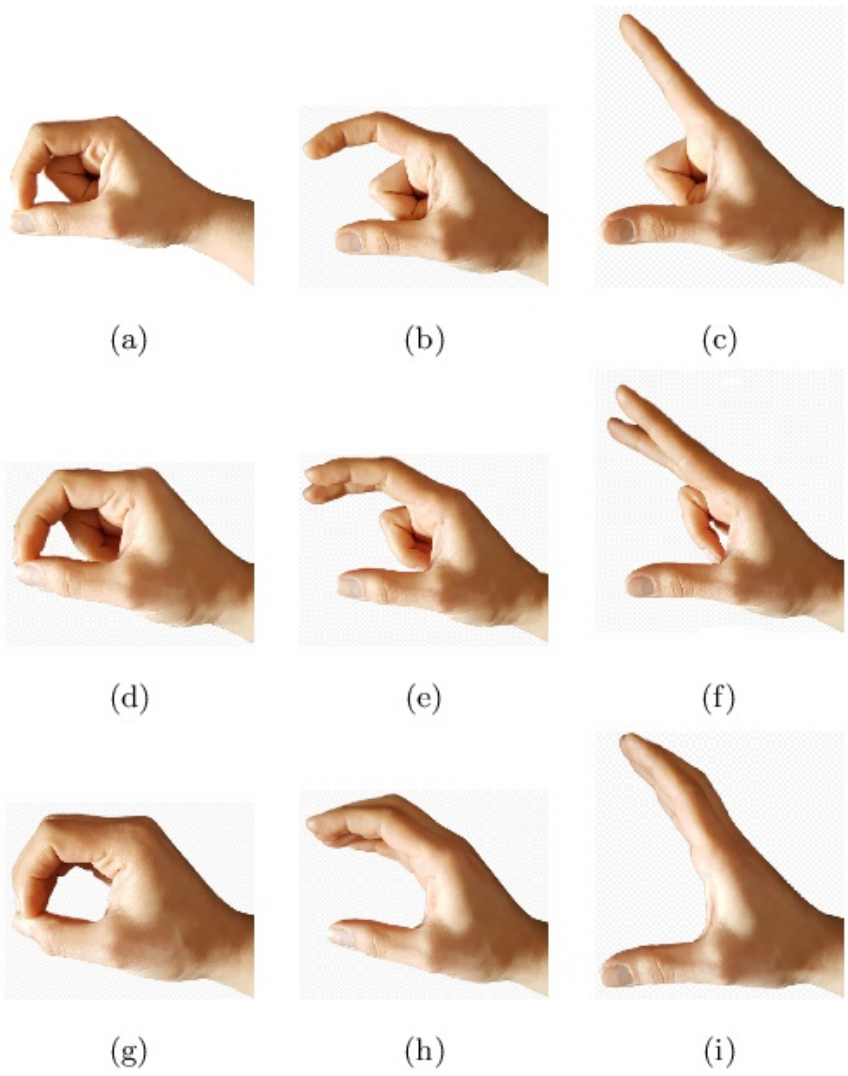

Figure 4.9: Snap shots of the hand's motion. a-c. Opposed thumb/index finger grip d-f. Opposed thumb/two finger grip g-i. Heavy wrap/large diameter

[57]. To build upon the work of Kadkhodayan et al. [45] the same grasp types were selected, and the investigation of the effect of the wrist movement variations was added. The three grasps are opposed Thumb-Index Finger grip, opposed Thumb-two Finger grip, and Heavy wrap-Large Diameter. Figure 4.9 shows the snapshots of the grasp types during flexing and extending fingers. The first two hand movements are precision grasps which mainly are used for manipulating a small object with fingertips. The third grasp is a power grasp and is mainly used for grasping large cylindrical objects. For simplicity the grasps were called "Index Finger-Thumb", "Two Fingers-Thumb" and "Large Diameter" grasp, to continue.

Since three-finger robotic hands and prosthetic hands are commonly used [58, 59, 60], the movement of the Index finger, Middle finger, and Thumb were studied in this work. The participants did the grasps repeatedly, which provided data from three dynamic hand movements.

In addition to the hand movements, we looked at the effect of the position of the wrist on the FMG. This can provide data to cover the last two parts of **objective 1** and the **objective 2**. To do this six static wrist positions were used to collect data. These positions included keeping the wrist in Extension, Flexion, Neutral, Pronation, Radial deviation, and Ulnar deviation. This study is a feasibility study regarding the investigation of the effect of the wrist position on the FMG signal and is a first step toward removing the wrist position effect. Thus, only the six static wrist positions following the work of Pan et al. [30] were included in this study, and wrist transition between the static positions was not considered. As the motion capture system was not able to see the markers on the fingers during the hand movements in Supination wrist position, this position was not included in the study. Figure 4.10 illustrates the wrist positions. The mentioned grasp types and wrist positions were demonstrated for the participants. After fixing their elbow and wrist position, they were asked to flex and extend their fingers and Thumb as if they were grasping objects of different sizes. The participants did not hold or squeeze any object. The effect of applying force on an object or surface is not investigated in this study since it is a feasibility study on the wrist movement effect on the signal. The participants were asked to do each grasp for 10 seconds. As there are three hand movements this adds up to 30 seconds in total. The participants repeat the hand movements 30 times. Since the sampling frequency of the band was set to 15Hz, the repetitions provided approximately 13500 data point for each wrist position. The dataset for each data collection session nearly included 81000 data points. Participants were asked if they need a rest every ten minutes. In addition, there was a mandatory rest halfway through the experiment for fifteen minutes. There were no limitations on the speed, and participants performed the motion at their natural speed. With the considerations mentioned above, the data collection session for each participant, including setup, rest between repetitions, and recording data, was approximately 3 hours

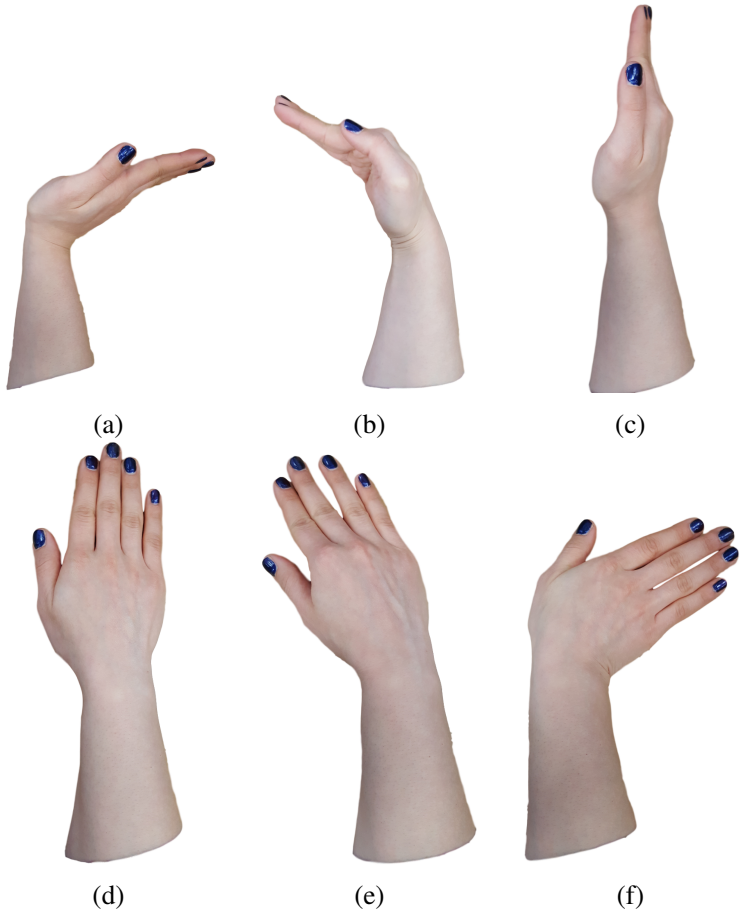

Figure 4.10: Snap shots of wrist positions. a. Extension b. Flexion c. Neutral d. Pronation e. Radial deviation f. Ulnar deviation.

long. It is worth mentioning that the fatigue has a lower influence on FMG signal than sEMG signal [37]. The collected data were saved for further processing in an offline setting.

4.6 Motion Data Processing

To investigate the FMG data and the motion of the hand movement, it is important to define a measure of the hand movement. In the partial prostheses hands usually the individual control of each finger joint is not provided, and the hand does not have the same kinematic of the real hand. As a result, if the finger joints are predicted, to control a prosthesis they need to be converted to the kinematics of the prosthesis to be able to control it. This motivated us to define a measure of the grasping movements. Kadkhodayan et al. [45] used the distance between the index fingertip and a reference point on the hand and the middle fingertip and

the reference point on the hand. This measurement can depend on the participant's body measurements. The distance for a tall person can be more from this distance for a short person. That motivated us to use a measurement that does not depend on the participant's body size. The angle between the index finger and thumb, and middle finger and thumb were selected (Figure 4.11).

The collected marker location data were used to calculate three vectors. The first one was defined as the vector starting from the thumb's MCP joint and ends at thumb's tip (V_{MT}). The second vector starts at thumb's MCP and ends at index finger's tip (V_{MI}). The last vector starts at thumb's MCP and ends at middle finger's tip (V_{MM}). These vectors were used to calculate the angle between the thumb and index finger (θ_{TI}), and the angle between the thumb and the middle finger (θ_{TM}). Figure 4.11 illustrates the angle between the middle finger and thumb and index finger and thumb. Formula 4.1 and formula 4.2 show the calculation of the angle for index finger and thumb, and middle finger and thumb.

$$\theta_{TI} = \tan^{-1}\left(\frac{|\vec{V}_{MT} \times \vec{V}_{MI}|}{\vec{V}_{MT}.\vec{V}_{MI}}\right) \tag{4.1}$$

$$\theta_{TM} = \tan^{-1}\left(\frac{|\vec{V}_{MT} \times \vec{V}_{MM}|}{\vec{V}_{MT}.\vec{V}_{MM}}\right) \tag{4.2}$$

The changes in the value of θ_{TI} and θ_{TM} were used as the measures of grasping motion for training and testing a regression model, and the FMG data was used as the regression model's input. Considering the six wrist positions and three hand movements there are 18 different states for θ_{TI}. As the middle finger is not moving in Index Finger-Thumb grasp, the data from this movement is not included in θ_{TM}'s data set. This provides 12 states for the investigation of θ_{TM}.

4.7 Summary

The chapter presented the experimental protocol and setup. The setup and protocol were designed to provide data, which can be analyzed to cover **both objectives**.

As FSRs had shown to be a reliable sensor for collecting FMG signal, an FMG data collection band was designed and made using 18 FSRs. The band was connected to a

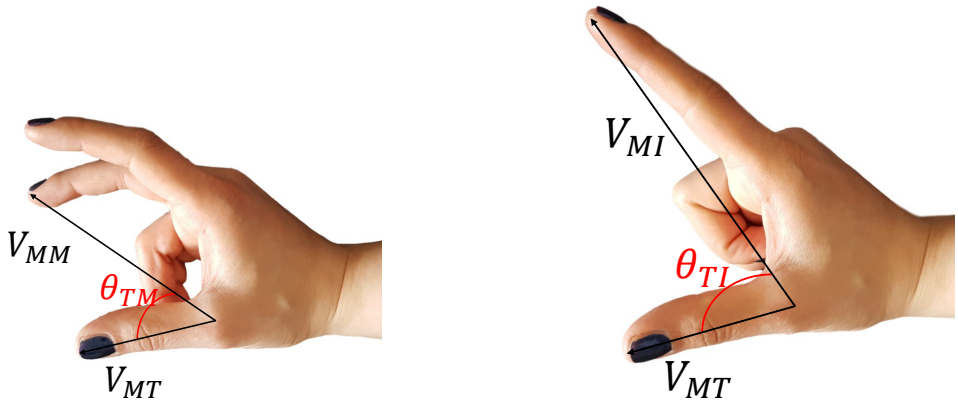

Figure 4.11: a. The angle between middle finger and thumb b. The angle between index finger and thumb

computer and sent the data to the computer over a serial connection. A motion capture system, including eight cameras and fifteen markers, was set up to track the movements of the hand and fingers. The motion capture system sent the data to the computer over a TCP connection. A costume program was coded in C# to collect synchronized data from the motion capture system and the FMG data collection band.

One of the goals of the study is to investigate the effect of static wrist position variation. Six wrist positions were selected to collect the data. To keep the participants' wrist in each wrist position and control the experiment a brace was designed and made. The participant's hand was fixed in each of the wrist positions and the data from the finger movements were recorded.

The experimental protocol was designed to investigate the effect of the wrist position on the signal while the fingers are moving. The movement of two fingers and thumb were considered. Three hand movements were selected. The participants were asked to flex and extend their fingers, in the specific hand movements, while their wrist was fixed in one of the six predefined wrist positions. This provides three dynamic hand movements and six static wrist positions.

The data collected from the band and the motion capture system was recorded and saved for further processing. The angle between thumb and index finger (θ_{TI}) and the angle between thumb and middle finger (θ_{TM}), were selected and defined as measures of hand

movement. In further investigations and to train and test the machine learning algorithms, the FMG data was used as the input of the system and the angle value was used as the output of the system. The next chapter will go over the data processing and data analysis methods to cover **objective 1**.

Chapter 5

Feasibility of grasping estimation in presence of wrist position variation

This chapter covers the data analysis methods, results, and discussion to cover **objective 1**. To predict the continuous movement, two approaches are studied. The first approach is suggested by the author, while the other one follows the common practice for estimation of hand movements in different wrist positions, which is using a classifier first to determine the wrist position.

5.1 Data analysis

For predicting grasp movements two approaches were explored and compared. The approaches are One-Step Regression and Two-Step Regression. The changes in the value of θ_{TI} and θ_{TM} were used as the target variable in the training and testing phases, and the FMG data was used as the predictor variable. All data processing and analysis were done in an offline setting. The tests were performed on a server running Cenots ver 6.9 equipped with four twelve-core (2 threads per core) Intel(R) Xeon(R) processors (E7-4860 v2 @ 2.60GHz) and 1000 GB RAM. To have a fair comparison between different models and approaches, all programs were run with a single core.

5.1.1 One-Step Regression

In the first approach, One-Step Regression, a single regression model was used for training the model and testing it, regardless of the hand movement or the position of the wrist. Both training and testing datasets included data from all static wrist positions and dynamic

Figure 5.1: The structure of One-Step Regression

hand movements. Four regression models, namely LR, SVR, NNR, and RF regression were trained, tested and compared to identify which one performs better toward the goal of this study. The data for each angle was studied independently. Figure 5.1 shows the structure of the One-Step Regression approach.

5.1.2 Two-Step Regression

Previous works on sEMG signal have shown that the movement of the wrist degrades the signal and there is a need to define separate models for different wrist positions [30, 5]. Pan et al. [30] indicated when sEMG is used with different models for different wrist positions, it is possible to estimate the continuous finger movements. The two-step regression approach was designed with an inspiration of their work. Comparing this approach and the one-step regression approach can indicate whether FMG needs different models for different wrist position, similar to sEMG. In addition, by including the two approaches we can roughly compare sEMG and FMG for the same application.

This approach consisted of a six-class classifier and six regression models corresponding to six wrist positions for each angle. At the first step, the data points belonging to each wrist position were gathered together. For each group, a regression model was trained. Then a classification model was trained to classify the wrist positions. To test a new data point, first, the classifier found the wrist position that the point belonged to, then based on the predicted wrist position the corresponding regression model was selected and used to predict the angle. Figure 5.2 illustrates the structure of the Two-Step Regression approach.

To choose the appropriate classification method for the second approach three classification methods were explored. As LDA and SVM with a Gaussian kernel have been used in the literature to classify wrist and hand movements using FMG [47, 39, 31], these two clas-

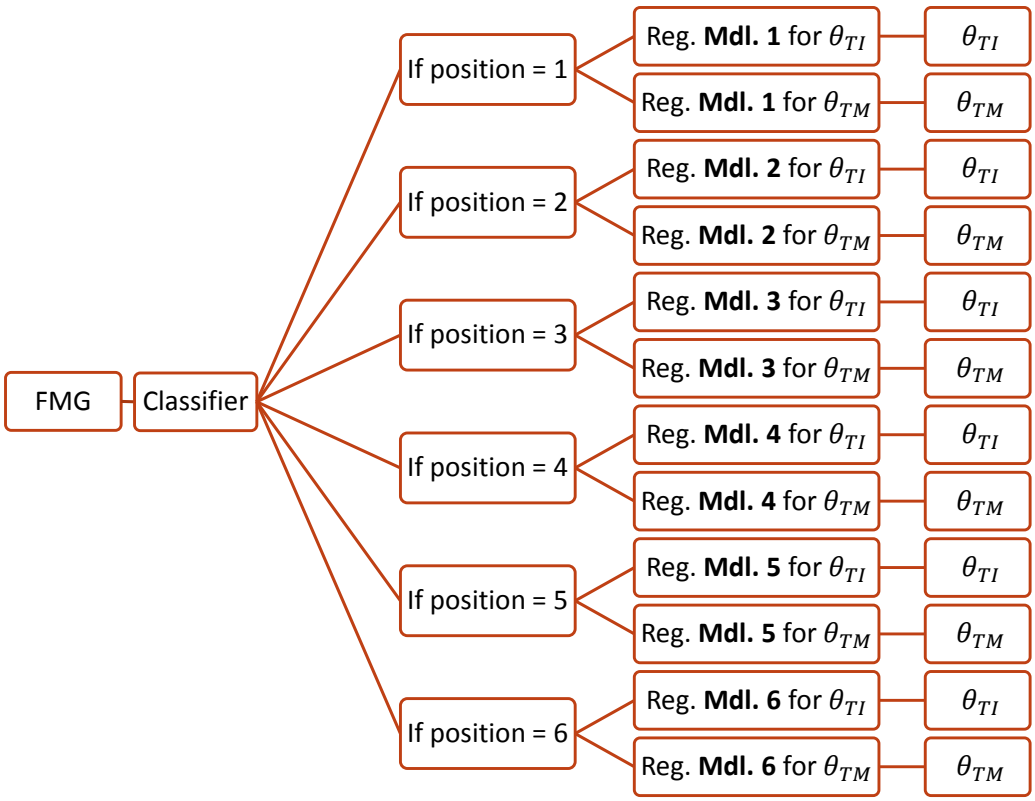

Figure 5.2: The structure of Two-Step Regression

sifiers were tested. In addition to those algorithms RF [49, 50] is introduced for classification using the FMG signal.

The result from the two approaches can indicate whether it is possible to use FMG signal for hand movement regression in different wrist positions.

5.1.3 Outcome measures

Each of the approaches was investigated separately for θ_{TI} and θ_{TM}. The data from each subject was analyzed independently. The data set includes thirty repetitions of each hand movement in each wrist position. A cross-repetition method was used for evaluating the performance. In a cross-repetition method, the data collected from a set of repetitions are left out as the testing dataset and were not used for the model optimization. To shape training and testing data set, for each approach, six repetitions out of thirty repetitions were randomly selected, without replacement and set out for testing and other twenty-four repetitions were used for training. This testing and training set definition means 20% of the

repetitions were used for testing and 80% for training. This was done five times, to make sure that each repetition has been in the test set at least once. The result is reported as an average among repetitions and participants. The coefficient of determination (R^2), the percentage root mean square error ($RMSE\%$), the average training time, and the estimated prediction time for a new data point were measured as ways to evaluate the performance of the modeling.

$$R^2 = 1 - \frac{\sum_{i=1}^{N} (y_i - y_i\prime)^2}{\sum_{i=1}^{N} (y_i - \bar{y})^2} \tag{5.1}$$

$$RMSE\% = \frac{\sqrt{\frac{1}{N}\sum_{i=1}^{N} (y_i - y_i\prime)^2}}{y_{max} - y_{min}} \times 100 \tag{5.2}$$

Formula 5.1 shows the calculation of R^2, and Formula 5.2 shows the calculation of $RMSE\%$ value. The expected value is shown with y, $y\prime$ shows the predicted value, $\bar{y}$ indicates the average of y in the test set and N indicates the number of data points in the test set. To measure the estimated prediction time for a new data point, the prediction time for the testing phase was measured and divided by the number of data points in the test dataset.

Concerning the Two-Step Regression approach, it is important to keep in mind that the evaluation measurements were calculated using the final output, which is the predicted value of θ.

The data set was scanned. If an angle data point was missing, due to the data corruption, the corresponding FMG data was ignored and the data point was removed. No other prepossessing was done on the FMG signal and the raw FMG data was used for classification and regression. The proposed algorithms were tested on θ_{TM} and θ_{TI} independently. Train and test data sets were the same in the one-step regression and two-step regression. The same sets were also used for analyzing the effect of reducing the size of the training dataset.

5.2 Results

Ten able-bodied subjects, six males and four females, age 23-41 participated in this study. The experiment received ethics approval from Simon Fraser University, and participants gave their written informed consent. The comparison between two approaches helps to identify the appropriate approach, among two for estimating continuous hand movement. Moreover, it helps to investigate the feasibility of using FMG for continuous hand movement prediction.

5.2.1 One-Step Regression

Table 5.1 shows the results for θ_{TI}. The $R^2_{\theta_{TI}}$ values for LR, SVR, NNR and RF were 0.694, 0.868, 0.813 and 0.872 respectively. The $R^2_{\theta_{TI}}$ value indicated that RF performed slightly better than SVR, and NNR, while it significantly outperformed LR. The RF algorithm was about four times faster than SVR and more than 49 times faster than NNR during the training phase. The RF algorithm is also significantly faster than SVR and NNR to predict the output for a new data point.

Table 5.2 indicates the results for θ_{TM}. The $R^2_{\theta_{TM}}$ values for LR, SVR, NNR and RF were 0.873, 0.941, 0.911 and 0.941 respectively. Looking at the result of θ_{TM} regression, it showed the similarity between SVR and RF, while RF was over two times faster than SVR during the training, and more than seven times faster during testing. RF also performs slightly better than NNR, and the NNR is about 33 times slower than the RF algorithm in both training and testing. The result confirms that the RF algorithm is a good alternative to the other three conventional algorithms for this research.

Figure 5.3 illustrates an example of predicting θ_{TM} using one-step regression approach with RF regression algorithm. Using RF regression R^2 value of 0.872 and 0.941 were obtained for θ_{TI} and θ_{TM} respectively.

5.2.2 Two-Step Regression

Based on the result of the first approach, RF was selected as the regression model. Table 5.3 indicates the result of the classifiers comparison. The accuracy of 85.01%, 95.55%, and 95.76% were obtained for LDA, SVM, and RF on average. RF algorithm was able to do the

Table 5.1: Regression algorithms comparison for θ_{TI}, One-Step Regression approach

	R^2	$RMSE\%$	Training Time (Minutes)	Estimated prediction Time (ms) for Each Sample point
LR	0.6945 ± 0.07	14.59 ± 1.71%	0.011 ± 0.012	0.0006
SVR	0.8680 ± 0.03	9.55 ± 1.07%	6.172 ± 0.946	1.097
NNR	0.8129 ± 0.06	11.29 ± 1.51%	72.925 ± 7.40	3.730
RF	0.8718 ± 0.03	9.40 ± 1.05%	1.487 ± 0.14	0.076

Table 5.2: Regression algorithms comparison for θ_{TM}, One-Step Regression

	R^2	$RMSE\%$	Training Time (Minutes)	Estimated prediction Time (ms) for Each Sample point
LR	0.8734 ± 0.05	8.98 ± 1.27%	0.008 ± 0.01	0.0006
SVR	0.9415 ± 0.02	6.12 ± 0.83%	2.35 ± 0.45	0.585
NNR	0.9110 ± 0.03	7.53 ± 0.97%	32.00 ± 3.38	2.449
RF	0.9411 ± 0.02	6.13 ± 0.84%	0.95 ± 0.08	0.076

classification marginally better than SVM, while it was 1.5 times faster, and it outperforms the LDA classifier. The result and training time confirm that RF algorithm can perform as an alternative to LDA and SVM to classify wrist position using FMG signal.

Figure 5.4 illustrates the RF algorithm's confusion matrix. The confusion matrix indicates that the Pronation and Radial wrist positions are more likely to be miss-classified as each other compared to the other wrist positions. This miss-classification can be a result of the small deviation angle during the Radial deviation, which was an average of 18° for the participants.

Table 5.4 indicates the average results of the second approach. The $R^2_{\theta_{TI}} = 0.874$ and $R^2_{\theta_{TM}} = 0.942$ were obtained. Figure 5.5 shows a sample of the target and predicted value using the two-step regression approach. The training and testing dataset were the same as Figure 5.3.

Figure 5.6 shows the average R^2 of two-step regression in six static wrist positions. The data were grouped into the wrist positions based on the result of the classifier.

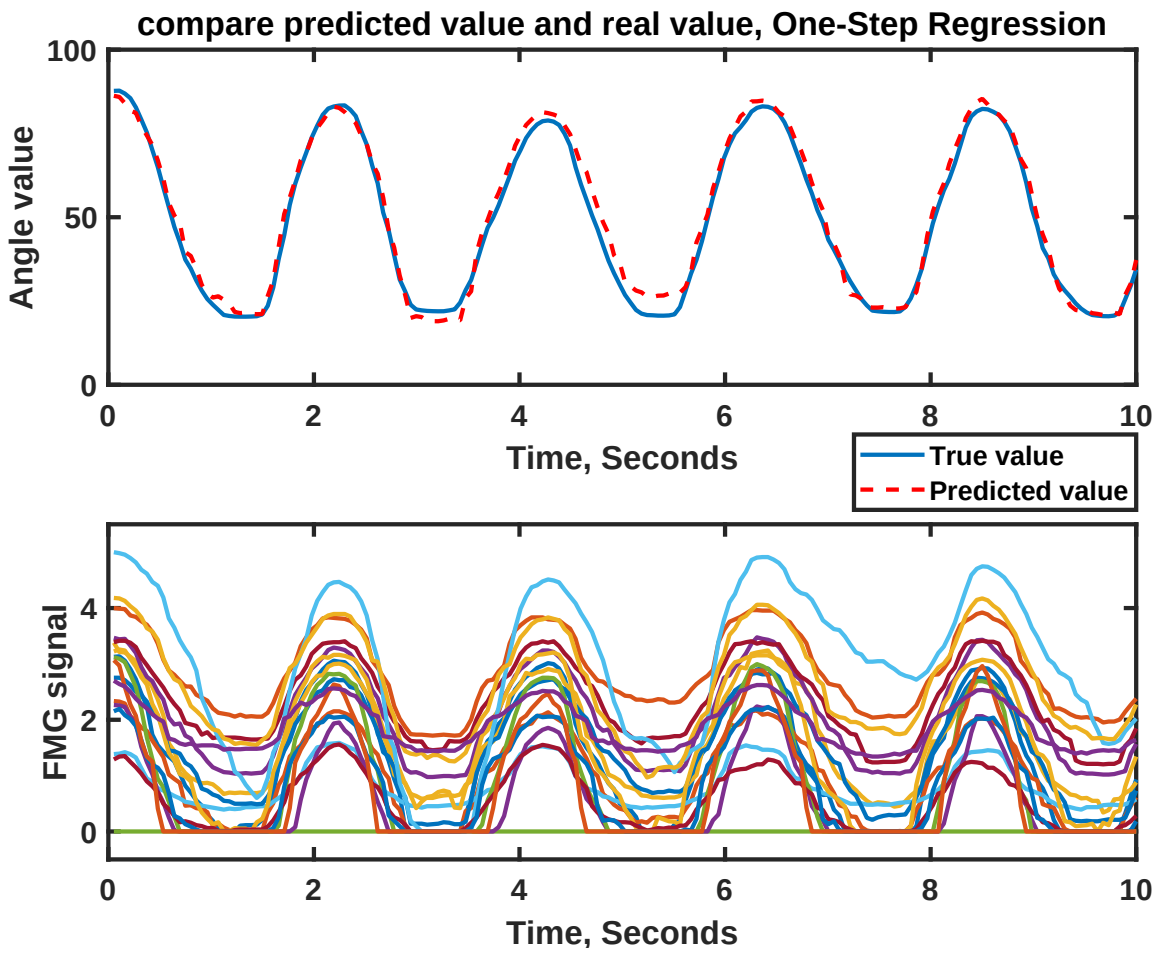

Figure 5.3: Predicted value with random forest regression and real value comparison, using One-Step Regression, for θ_{TM},subject #10, repetition #19,large diameter grasp, in pronation wrist position

The similarity in the average $R^2_{\theta_{TI}}$ and $R^2_{\theta_{TM}}$ from the two approaches indicate the potential of equivalency of the two approaches. Two one-sided t-test (TOST) [61] to test the equivalence was run on the $R^2_{\theta_{TI}}$ and $R^2_{\theta_{TM}}$ to compare the two approaches. The value of the level of significance was set to 0.05 ($\alpha = 0.05$), the lower limit of the equivalence interval was set to -0.015 and the upper limit of the equivalence interval was set to 0.015. The null hypothesis was set as: $(\mu_{R^2_{one-step}} - \mu_{R^2_{two-step}}) > 0.015$ or $(\mu_{R^2_{one-step}} - \mu_{R^2_{two-step}}) < -0.015$, and the alternative hypothesis was set as: $-0.015 < (\mu_{R^2_{one-step}} - \mu_{R^2_{two-step}}) < 0.015$. The test resulted in $p < \alpha$ for both $R^2_{\theta_{TI}}$ and $R^2_{\theta_{TM}}$, which rejects the null hypothesis. Furthermore, the confidence interval of the difference falls entirely inside the equivalence

Table 5.3: Classification algorithms comparison for classifying six wrist positions

	Accuracy	Sensitivity	Specificity	Time (Second)
LDA	85.01 ± 9.55%	90.65 ± 11.06%	97.87 ± 3.22%	0.10 ± 0.07
SVM	95.55 ± 4.41%	97.46 ± 4.71%	99.52 ± 0.78%	58.82 ± 33.26
RF	95.76 ± 4.37%	97.42 ± 4.48%	99.45 ± 0.92%	38.77 ± 3.91

Table 5.4: The results of Two-Step Regression approach

	Classification Accuracy	R^2	$RMSE\%$	Training Time (Minutes)	Estimated prediction Time (ms) for Each Sample point
θ_{TI}	95.76 ± 4.38%	0.8744 ± 0.03	9.31 ± 1.07%	2.498 ± 0.179	68.174
θ_{TM}	96.45 ± 3.91%	0.9424 ± 0.02	6.06 ± 0.87%	1.665 ± 0.117	52.682

limits. This indicates the results from the two approaches are equivalent and they are not different from each other.

The result indicates that the second approach had a similar performance to the first approach while it was more than 1.5 times slower than the one-step regression approach in training phase and significantly slower during the prediction of a new data point. The results suggest that one regression model for each angle (θ_{TI} and θ_{TM}) can predict the angle value in the presence of variations of the position of the wrist. Subsequently, the first approach was selected to investigate the effect of the wrist position variation in chapter 6.

5.3 Discussion

The FMG signal was investigated for continuous hand movements estimation, with ten able-bodied participants. Concerning the goal of the study, two different methods were explored. The first was using a regression algorithm to predict the grasping movements; and the second was using a classification prior to the regression algorithm and six regression models corresponding to the wrist positions. The angle between Index finger and Thumb (θ_{TI}) and Middle finger and Thumb (θ_{TM}) were selected as the measures of the grasping movement.

Based on the presented result the two approaches had similar performance. The similarity between the two approaches can show that if enough information from different wrist positions is provided for the regressing model, it would be able to do the hand movement

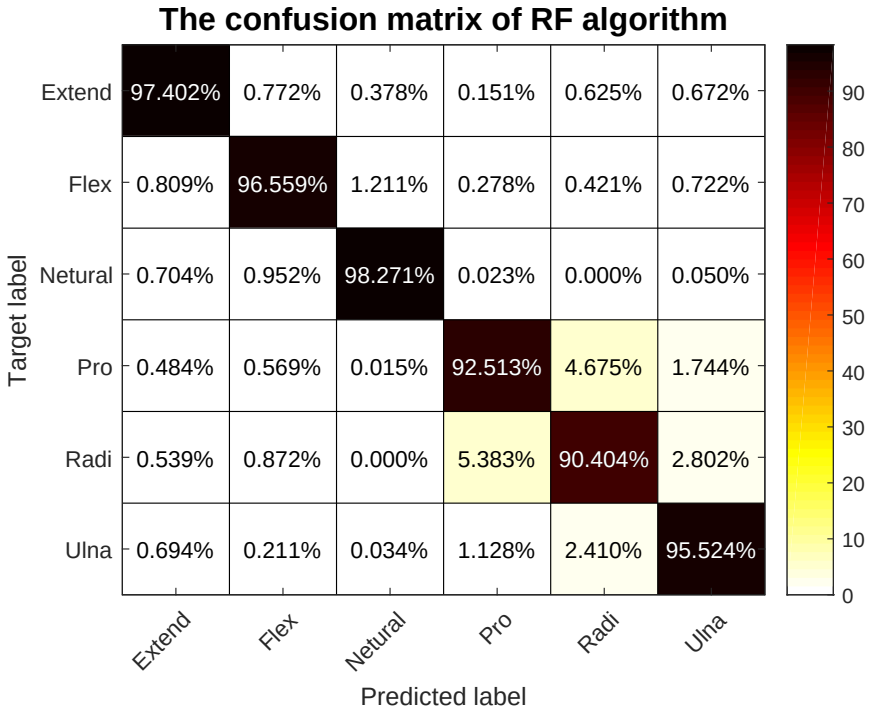

Figure 5.4: The confusion matrix of RF algorithm

estimation with a good accuracy. The second approach is slower than the first approach, during both training and prediction phases. The time difference can come from the complexity of the model. In the first approach, only two regression models need to be trained whereas in two-step regression approach a classifier and 12 regression models need to be trained. To predict the output of a new data point with one-step regression, the data point only goes through a regression model. However, in two-step regression, first, the data point goes through a classifier and then a regression model. One regression model for the θ_{TI} angle and a regression model for θ_{TM} were able to estimate the continuous hand movement with an average R^2 of 0.906 and $RMSE\%$ of 7.77%. Pan et al. [30] were able to predict continuous finger movement in static wrist positions using sEMG with an average R^2 about 0.8. They used a switching regime approach and trained different regression models for different wrist positions. In addition, Pan et al. [30] estimates the testing time for a new data point to be 53.011ms. Our work shows that FMG can predict a new data point in approximately 0.076 ms during the first approach. The present study implies that the FMG signal demonstrates comparable performance to sEMG in the same application, while there

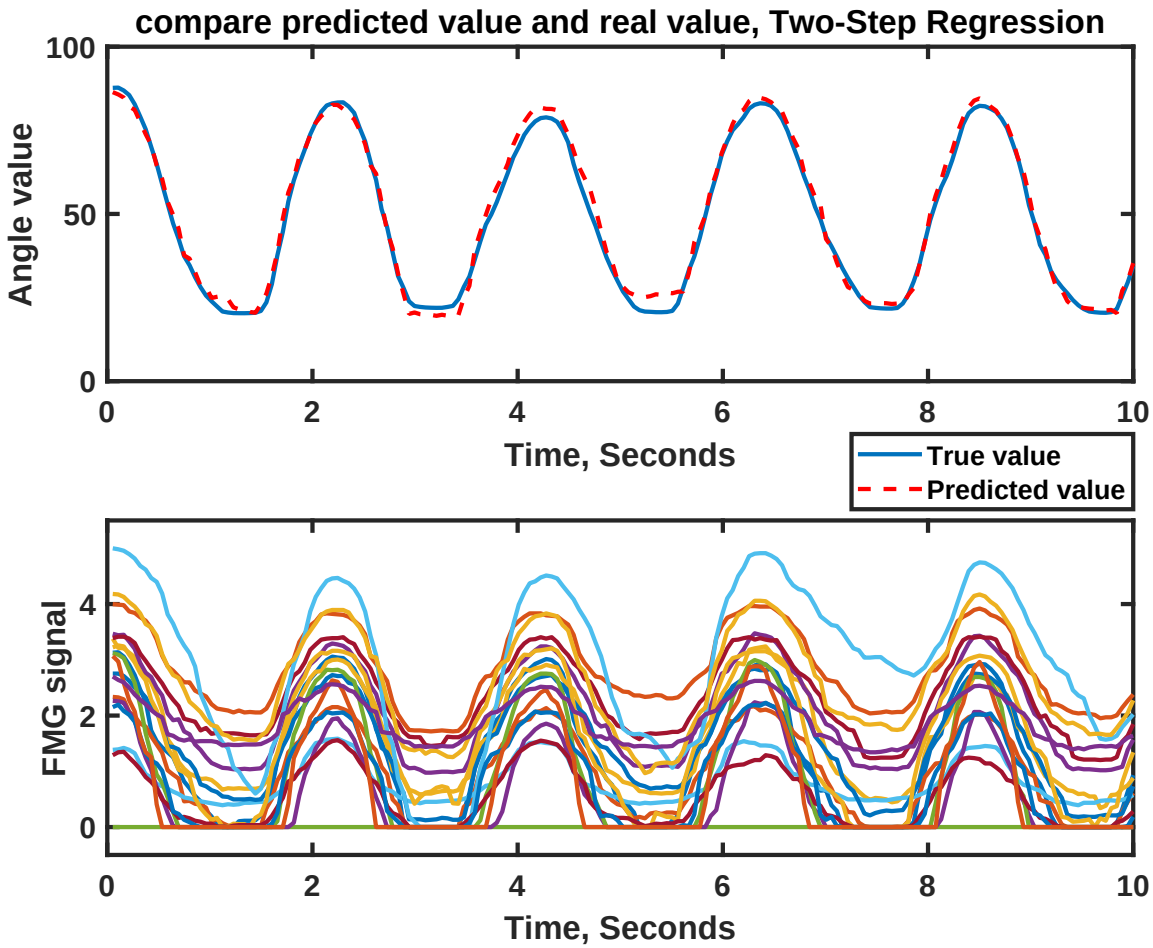

Figure 5.5: Predicted value with random forest regression and real value comparison, using Two-Step Regression, for θ_{TM},subject #10, repetition #19,large diameter grasp, in pronation wrist position

is no need to have different models for different wrist positions, as long as the data from different wrist positions are provided during the training.

With respect to one step regression, the RF algorithm was able to have comparable results to SVR, and NNR while it was faster. The training time of the SVR and NNR algorithm is sensitive to hyper-parameter optimization process. The NN package of MATLAB was used, which need one parameter to be optimized. The parameter is the value of bias in the Radial Basis Neural Network structure of the first layer. Using SVR, the value of the kernel scale was optimized. However, RF algorithm is not sensitive to optimization of the hyper-parameters [49, 50]. The default values of training in MATLAB were used, thus the training time was shorter. In addition to that, the time of the training using the RF

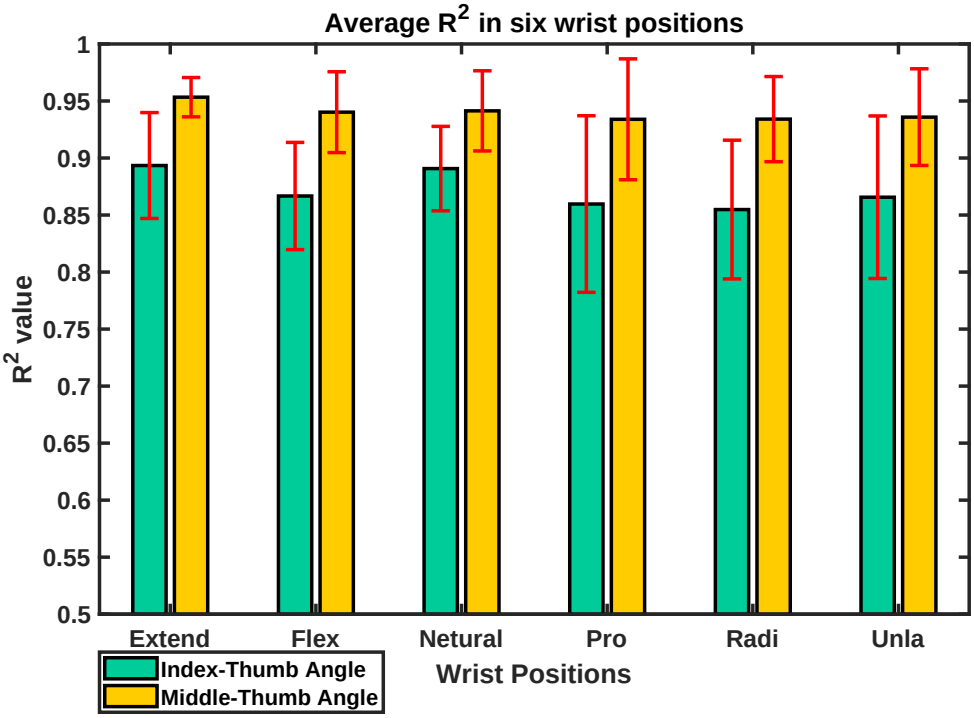

Figure 5.6: The average R^2 of two-step regression in six static wrist positions

algorithm was not sensitive to the size of the dataset. As mentioned in "Motion Data Processing" θ_{TM} included 12 states and θ_{TI} included 18 states. The time of the training using the RF algorithm was 1.49 and 0.95 minutes for θ_{TI} and θ_{TM} respectively, and the training time of SVR algorithm was 6.17 and 2.35 for the angles respectively. This training time indicated that in the RF algorithm by increasing the size of the dataset the training time did not increase drastically. The training time using SVR algorithm for θ_{TI} is over 2.5 times more than the training time for θ_{TM} with fewer data points. Regarding the NNR algorithm, the training time of the θ_{TI} is about twice the training time of θ_{TM}. The training times indicated the sensitivity of the SVR and NNR models to the size of the training dataset. The result for θ_{TM} dataset also indicates that the RF regression was a good alternative for the other commonly used regression models for the goal of this paper.

The results indicated, independent of the approach, θ_{TI} has a lower R^2 and higher $RMSE\%$ than θ_{TM}. This result can be justified by looking at the hand movements that are included in the dataset for each angle. As it was mentioned before, since the Middle finger is not moving in the Index Finger-Thumb movement, this movement is not included in the

dataset of θ_{TM}. The Index Finger-Thumb movement is more challenging to predict than the other two hand movements. The FMG band is placed on the forearm near the wrist. In this specific location, the finger controlling and wrist controlling tendons and muscles are passing. These tendons and muscles are responsible for the movements of the fingers, thumb, and wrist. The following muscles or tendons connected to them are passing under the band: The Flexor Carpi Radialis, Palmaris Longus, Flexor Carpi Ulnaris, Extensor Carpi Radialis Brevis, and Extensor Carpi Ulnaris which are responsible for controlling the wrist; Flexor Digitorum Superficial, Extensor Digitorum Communis, and Flexor Digitorum Profundus that are responsible for controlling the fingers; Extensor Digiti Minimi which is responsible for controlling the little finger; Extensor Indicis Proprius that is responsible for extending the index finger; Abductor Pollicis Longus and Extensor Pollicis Brevis that are responsible for controlling the thumb.

In a fixed wrist position, which minimizes the effect of the wrist-controlling tendons and muscles on the sensors, the finger-controlling and thumb-controlling tendons and muscles have the most effect on the changes of the sensors' reading and the signal. This means the changes in the sensors' readings on the band are mostly caused by these tendons and muscles.

Keeping three hand movements in mind, in the index finger-thumb movement only index and thumb were moving. This means only the tendons and muscles that are responsible for controlling the thumb and Index fingers were affecting the signal. While in two finger-thumb movements the tendons and muscles responsible for moving middle finger were influencing the signal as well. In the large diameter grip, all the fingers were moving, and there were more changes in each sensor's reading in this movement. Every one of the sensors in the band can provide information for the machine learning algorithm. Since in the two-finger thumb movement and large diameter grip more sensors are influenced, more information is provided for the machine learning algorithm. This results in a better performance in estimating the angle in these two hand movements. Despite the facts mentioned above, it is worth noticing that both methods were able to estimate θ_{TI} with an R^2 more than 0.8.

5.4 Summary

The data collected from the motion capture system was used to calculate the angle between index finger and thumb (θ_{TI}) and middle finger and thumb (θ_{TM}). The angles were used as the target value for the machine learning algorithms.

To predict the grasping movement using FMG data two approaches were investigated. The first approach was to use one regression model to estimate the angle, without considering the wrist position or the grasp type. Four regression algorithms were investigated to find the suitable regression algorithm for estimating the hand movement continuously, in this work. The investigation of different regression models covers the first part of the **objective 1**. The second approach included a classifier to classify the wrist positions and six regression models corresponding to each wrist position. The regression model was selected based on the result of the first approach and three classifiers were compared to get the best classifier among three to classify six wrist positions. The comparison between the classifiers covers the second part of the **objective 1**. The two approaches were compared together for the goal of the study. The result of each approach validated the possibility of using FMG signal for hand movement regression in different wrist positions, hence it covers the last part of **objective 1**.

The first approach, One-Step regression, was able to get R^2 values of 0.8718 and 0.9411 for θ_{TI} and θ_{TM}, respectively using an RF regression algorithm. The second approach, Two-Step regression, was able to get an R^2 values of 0.8744 and 0.9424 for θ_{TI} and θ_{TM}, respectively, while it was more than two times slower than the first approach during the training phase and significantly slower in testing. While the two approaches had similar R^2 values, the training and testing time were motivations to select the first approach to estimate the continuous hand movements, in this study. A rough comparison between the result from the first approach with the result of the similar work using sEMG, indicated that FMG has a comparable performance to sEMG, while it can be faster in testing a new data point.

In addition, the output measures of the system indicated that the system can predict the value of θ_{TM} more accurate than θ_{TI}. Looking at the hand movements included in the

dataset of each angle, and the hand anatomy presented in section 2.1, we can see that this difference is a result of the number of the sensors that are affected by tendons and muscles during each hand movement. It is worth noting that the calculated $R^2_{\theta_{TI}}$ is greater than 0.8 in all cases.

The next chapter will cover the data analysis, results and discussions to cover **objective 2**.

Chapter 6

Investigation of the effect of wrist movement in prediction

Chapter 5 validated the usage of FMG signal for continuous hand movement prediction. The results and discussions presented in the previous chapter led the author to select the one-step regression approach to estimate the hand movement in presence of the wrist position variations. The results of the first approach are selected to investigate the effect of the wrist position variations of the estimation. The presented data analysis, results, and discussion here cover **objective 2**.

6.1 Data analysis

To fit an amputee person with a prosthesis device the person goes through a set of practice and training sessions with their rehabilitation team. The training sessions for externally powered prostheses include training a prediction model to control the device. Previous researches have shown that for partial hand amputees it is important to include data from different wrist positions in the training process [5, 30, 14]. Moreover, to have a comfortable process it is desirable to spend less time setting up the device. To reduce the time of the training process for the prediction model, without ignoring the effect of the wrist position two questions were answered: i) is it possible to only include one wrist position in the training process using FMG? ii) If it is necessary to include more than one wrist position, can we train on less than six wrist positions without a significant effect on results?

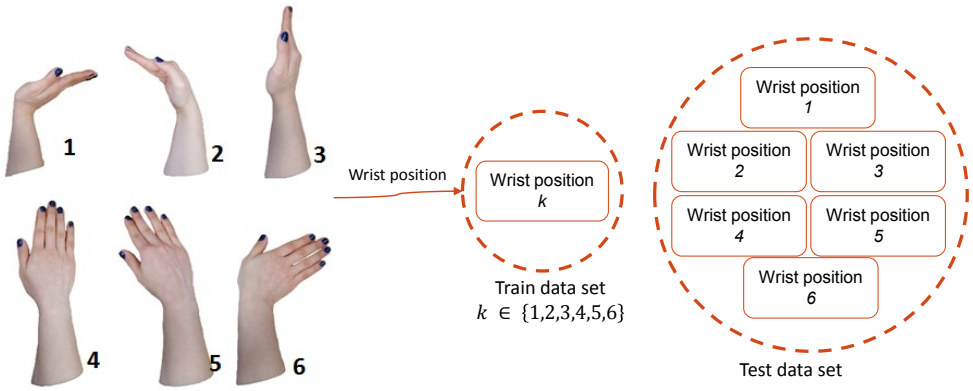

Figure 6.1: Including one wrist position in training phase and including all in testing

The effect of the variation of the wrist positioning on the performance of the model was investigated. The investigation was done to determine if it is possible to train on a fixed wrist position and predict the hand movement in different wrist positions. In addition to that, the minimum number of wrist positions that need to be included in the training phase was examined. The identification of the minimum number of wrist positions that should be included in the training data set helps to reduce the training data collection time. The same server computer as in chapter 5 is used to run the tests.

6.1.1 Analysis of the Effect of the Wrist Position Variation

As it was mention in section 2.2.2, the movement of the wrist can affect the performance of the prediction. To analyze how the wrist position affects the performance first, data from one wrist position was included in the training phase, while data from all six positions were included in the testing set. Each wrist position was used in the training phase at least once (figure 6.1). The result of this part can confirm whether it is necessary to train on different wrist positions or not. Then data from six positions were included in both the training and testing phase. One-way ANOVA and Tukey HSD test for post-hoc analysis were used to compare including six wrist positions, and including just one of the wrist positions in the training dataset.

After that, the possibility of including less than six positions in the training phase, and the inclusion of all six positions in the testing phase was investigated. To do this the data of one or a set of wrist positions were left out of the training dataset, while their data were

included in the testing dataset. The reasoning behind it was if for instance, the data in the Neutral wrist position was similar to the data in the Pronation wrist position, it would be possible to include just the data from one of those wrist positions in training data while including both of them in the testing phase.

Five cases were considered. In each case, one, two, three, four or five static wrist positions were removed from the training set, while their data was included in the test dataset. In case of removing two to five wrist positions, all combinations of removing wrist positions from the training data were considered. For instance, in case of removing two wrist positions, 15 combinations needed to be considered. Considering all combinations provides 62 different options in total. The performance of each option was calculated and compared to the performance of the system when all six positions were used for the training phase. One-way ANOVA and Tukey HSD test were used to determine which combinations do not have a statistically significant difference with including all six positions in the training dataset.

In all statistical analysis a confidence interval of 95% was considered ($\alpha = 0.05$). The statistical significance test was run on θ_{TI} and θ_{TM} independently. For each angle, the statistic tests were run on two outcome measures, namely coefficient of determination (R^2), and the percentage root mean square error ($RMSE\%$). The combinations that did not demonstrate a statistically significant difference with including six wrist positions in the training test were identified for each angle, and each outcome measure. The identified combinations that were overlapped between two angles, and within the two outcome measures, were selected as the combinations that can be used instead of including all wrist positions, without influencing the performance of the prediction.

6.2 Results

The resulted R^2 and $RMSE\%$ values from the one-step regression approach are selected for this investigation. Each angle is investigated independently.

6.2.1 Analysis of the Effect of the Wrist Position Variation

All the possible combinations of removing one or more wrist positions from the training dataset were explored. Each combination was compared to the case of including all the wrist positions in the training dataset.

Table 6.1 and figure 6.2 indicate the result of including only one wrist position in the training dataset. As the result indicates training on only one wrist position can notably decrease the R^2 value and increase the $RMSE\%$. In all cases for both θ_{TI} and θ_{TM} the statistical analysis for R^2 and $RMSE\%$ resulted in, $p \ll \alpha$. The resulted p-value means we cannot conclude that there were no statistically significant differences between including all six positions in the training dataset or just including one wrist position. The result can confirm that including more than one wrist position in the training dataset is necessary, to predict continuous hand movement in the presence of wrist position variations.

After that by comparing all the different options for removing wrist positions from the training dataset (the result of different options are provided in A.1), the positions that can be removed, without significant influence on the prediction result are found. In case of removing one of the wrist positions from the training dataset, four options resulted in a p-value of more than 0.05. The $p > 0.05$ indicates that by removing any of these four wrist positions, no statistically significant difference can be established between the calculated R^2 and $RMSE\%$ with the values calculated with including all the six positions in the training dataset. Table 6.2 and figure 6.3 present the result of the wrist positions that need to be included in the training dataset and their corresponding R^2 and $RMSE\%$ value. The results indicated that the Extension, Pronation, Radial, or Ulnar wrist position can be removed from the training dataset. The full result of the statistical analysis of each angle, with R^2 and $RMSE\%$, is provided in Appendix A.2, which is the pair-wise comparison between all the 62 combinations and including all six wrist position in the training dataset. In addition, a sample of the FMG signal in different hand movements and wrist positions is provided in the Appendix. Appendix A.3 indicates that despite notable differences between some wrist positions in a hand movement, for example, Extension and Pronation wrist positions, there are similarities in others, like Pronation and Ulnar deviation.

Table 6.1: The result of including one wrist position in the training dataset

Included Wrist positions in training dataset	θ_{TI}		θ_{TM}	
	R^2	$RMSE\%$	R^2	$RMSE\%$
Extension, Flexion , Neutral, Pronation, Radial , Ulnar	0.872 ± 0.034	9.402 ± 1.052 %	0.941 ± 0.021	6.133 ± 0.843 %
Extension	0.412 ± 0.230	19.90 ± 2.79 %	0.566 ± 0.304	15.740 ± 4.460 %
Flexion	0.553 ± 0.345	22.64 ± 4.16 %	0.436 ± 0.339	18.359 ± 4.007 %
Neutral	0.550 ± 0.214	20.70 ± 3.50 %	0.593 ± 0.163	16.067 ± 2.818 %
Pronation	0.372 ± 0.160	17.56 ± 2.73 %	0.700 ± 0.170	13.533 ± 2.924 %
Radial	0.231 ± 0.157	17.45 ± 2.60 %	0.631 ± 0.203	15.027 ± 3.305 %
Ulnar	0.412 ± 0.277	18.10 ± 3.66 %	0.641 ± 0.277	14.120 ± 3.550 %

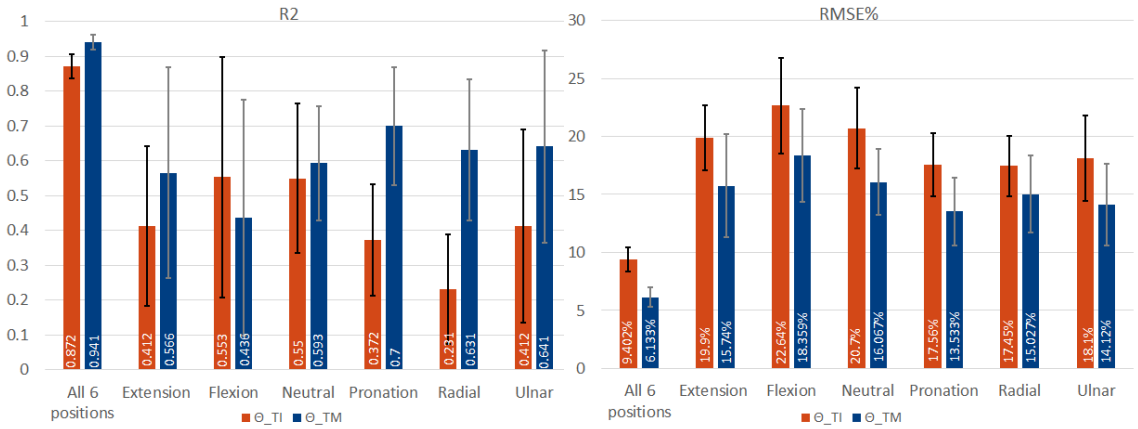

Figure 6.2: The result of including one wrist position in the training dataset

Table 6.2: The minimum number of the wrist positions that need to be included in the training dataset

Included Wrist position in training dataset	θ_{TI}		θ_{TM}	
	R^2	$RMSE\%$	R^2	$RMSE\%$
Extension, Flexion , Neutral, Pronation, Radial , Ulnar	0.872 ± 0.034	9.402 ± 1.052 %	0.941 ± 0.021	6.133 ± 0.843 %
Flexion , Neutral, Pronation, Radial , Ulnar	0.821 ± 0.056	11.072 ± 1.375 %	0.901 ± 0.051	7.810 ± 1.575 %
Extension, Flexion , Neutral, Radial , Ulnar	0.842 ± 0.046	10.432 ± 1.362 %	0.927 ± 0.034	6.748 ± 1.221 %
Extension, Flexion , Neutral, Pronation, Ulnar	0.845 ± 0.046	10.320 ± 1.343 %	0.925 ± 0.039	6.797 ± 1.187 %
Extension, Flexion , Neutral, Pronation, Radial	0.832 ± 0.051	10.722 ±1.238 %	0.919 ± 0.039	7.239 ± 1.070 %

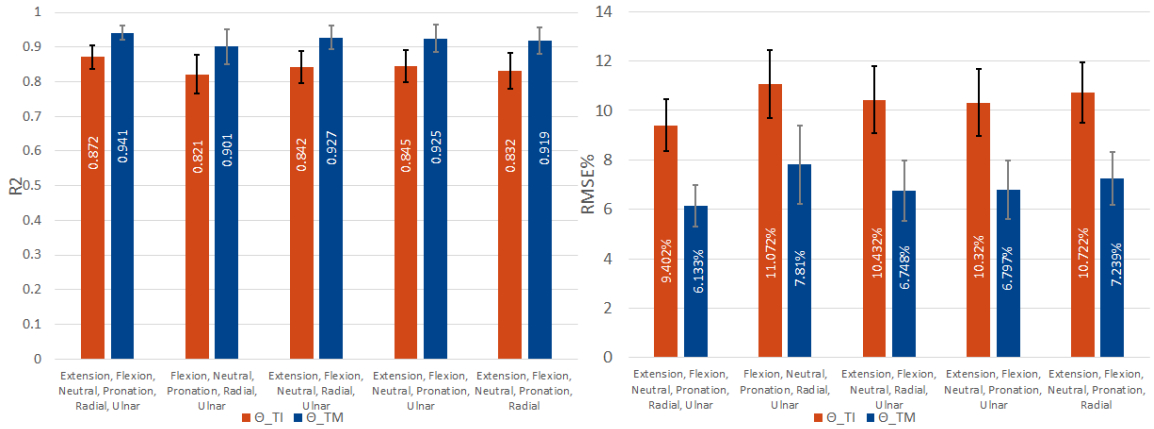

Figure 6.3: The minimum number of the wrist positions that need to be included in the training dataset

6.3 Discussion

By considering the effect of the wrist position variation, the study demonstrated a more comprehensive approach compared to the work of Kadkhodayan et al. [45] and took one step closer to a practical case. Adewuyi et al. [5] investigate the possibility of training the system on one wrist position and use it with variations in the position of the wrist, using sEMG signal. Their result indicated that the variation of the wrist position could have a negative effect on the performance of the model. Our result shows that the same effect can be observed in the FMG signal. If the system was only trained on one wrist positioning, it was not able to predict the continuous hand movement accompanied with wrist position variation with an average R^2 more than 0.6. The resulted R^2 value emphasizes the importance of including more than one wrist positions in the training data set.

Our further investigations revealed that it is possible to include five wrist positions in the training dataset and include all six positions in the testing phase. In other words, it is possible to remove Extension, Pronation, Radial, or Ulnar wrist position from the training dataset, without any statistically significant effect on the performance of the model. This provides four options for the training dataset, that include five wrist positions instead of six wrist positions (Table 6.2, row 2-5). In the present study, data collection from each wrist position was approximately 20 minutes long. Thus, by training on five wrist position instead of six, the data collection process reduces by 20 minutes. This shows that the FMG signal

has the potential to have a shorter setup time for a prosthesis device, without ignoring the effect of the wrist position variation on the signal.

The Tukey HSD test was run to do a pairwise analysis of the four options, which provided six combinations. The results showed $p > 0.05$ in all six combinations. The p-value indicated no statistically significant differences could be established between the four options. The statistical test does not necessarily mean that they have equivalent performance. However, it indicates that FMG has the potential to use any of alternative four options without degrading the performance of the system.

6.4 Summary

After identifying the proper methods for estimating the continuous hand movements, the effect of the wrist position variations was investigated. At first, the possibility of training the system on only one wrist position was investigated. The result demonstrated that it is not possible to estimate the grasping movement in different wrist positions if only one wrist position is included in the training phase, irrespective of the included wrist position.

Then one or more wrist positions were removed from the training data set while their data was included in the testing data set. This helped to investigate the possibility of reducing the number of wrist positions during training. The result indicated that it is possible to remove one wrist position (Extension, Pronation, Radial, or Ulnar wrist position) from training data while all wrist positions are included in testing data, with no statistically significant effect on the calculated R^2 and $RMSE\%$ result.

The outcomes and discussion of this chapter covered the investigation of the effect of the wrist position variation on the prediction and possibility of reducing the number of the wrist positions during training, thus it covers **objective 2**. Next chapter will summarize and conclude the remarks and results of the project. In addition to that, the suggestions for future works are presented in the next chapter.

Chapter 7

Conclusion

This chapter summarizes the findings and the objective of the thesis. Moreover, the suggestion to continue the work in the future are presented in this chapter.

7.1 Conclusion

In this study, the FMG signal was introduced and explored to provide continuous hand movement prediction toward controlling partial hand prosthesis. With having the importance of the effect of the wrist movement on the performance of the grasping movement prediction in mind, the effect of the wrist movement on the FMG signals performance during predicting continuous hand movement was explored. To the author's best knowledge this is the first work that considers the effect of the wrist movement on the performance of the FMG during continuous hand movement prediction.

Objective 1 of this work was to explore different regression models for continuous hand movement prediction, and different classification models for wrist position classification using the FMG signal. In addition, validate the usage of FMG signal for continuous hand movement prediction. To cover this objective two approaches were defined and examined for predicting continuous hand movement in the presence of different wrist positioning. The first approach was to use one regression model for grasping movement prediction, irrespective of hand movements and wrist positions. During the second approach, with an inspiration from the literature on sEMG signal, first, a classifier determined the wrist position that participant was in and after that, a regression model, trained for that wrist position, was used to predict the measures of the grasping movement. The two approaches had a similar

performance, while the first approach was significantly faster than the second approach. This indicates one regression model with adequate training data was able to predict the grasping movement, with an average R^2 of 0.906, while it was able to predict the angle for a new data point in less than 1 ms. The exploration of different regression models revealed that between the four regression models tested on the data, SVR and RF had similar performance, while RF was faster during both training and testing. In comparison between different classifiers, the accuracy of different algorithms shows that the six wrist positions are distinguishable, and all three presented classifiers had an accuracy higher than 80%. The training time of the RF algorithm makes it a good alternative for this classification. The experiment with the one-step regression and two-step regression can validate the usage of FMG signal for continuous hand movement prediction. The testing of the two approaches showed that in contrast with sEMG, which literature shows it needs a classifier prior to the estimation, the FMG signal can estimate the continuous movement with one regression model for each angle. Moreover, FMG signal with an RF regression model has the potential to do the prediction in a real-time setting.

Objective 2 of the thesis was to investigate the effect of the wrist position on the prediction and the possibility of reducing the number of wrist positions during training. The effect of the variations in the wrist position was investigated in chapter 6. The result concluded that by including only one wrist position in the training dataset, it is not possible to estimate the hand movement in different wrist positions. The same effect was observed in prediction with sEMG signal before [5]. It is necessary to include at least five wrist positions (Extension, Pronation, Radial, or Ulnar wrist position can be removed, table 6.2) in the training dataset to be able to predict continuous hand movement in different wrist positions.

In short, the presented study indicates the potential of FMG signal to be used as a control technology to provide continuous hand movement control for partial hand amputees.

7.2 Future Studies

As this work was a feasibility study, the data from each participant was collected in one session. Thus, the repeatability of the results during different sessions has not been investi-

gated, and it needs to be studied in future works. It is expected to have a repeatable result if the sensor placement between sessions is kept uniform. This can be achieved by designing a device that guides the user to put it back on similar to previous sessions. Future works can investigate the possibility of improving the performance by adding feature extraction from the FMG signal and studying different machine learning approaches for regression. Additionally, more hand movements, as well as random hand movements, can be included in the study as the number of the hand movements covered in this study were limited to three. To continue the work in the future, it is essential to test the ability of the signal to perform grasping movement regression, while the wrist is not constrained to specific angles and include a continuous wrist movement estimation in the algorithm if it is needed. It is also necessary to test the signal to control a simulated hand or a robotic hand gripper in real-time. In addition, the effect of the FMG band placement on the limb as well as the effect of the user's fatigue on the performance of the system should be investigated. Also, the effect of object handling, the resistance from holding and squeezing an object, and the drift of signal during long hours of using should be investigated. At last, it is important to test the result of the study with partial hand amputee participants and test the potential and limitations of the signal and the algorithm.

Bibliography

[1] Kathryn Ziegler-Graham, Ellen J MacKenzie, Patti L Ephraim, Thomas G Travison, and Ron Brookmeyer. Estimating the prevalence of limb loss in the united states: 2005 to 2050. *Archives of physical medicine and rehabilitation*, 89(3):422–429, 2008.

[2] Nadezhda Gavrilova, Aram Harijan, Sharon Schiro, Charles Scott Hultman, and Clara Lee. Patterns of finger amputation and replantation in the setting of a rapidly growing immigrant population. *Annals of plastic surgery*, 64(5):534–536, 2010.

[3] Ilario Imbinto, Carlo Peccia, Marco Controzzi, Andrea Giovanni Cutti, Angelo Davalli, Rinaldo Sacchetti, and Christian Cipriani. Treatment of the partial hand amputation: an engineering perspective. *IEEE reviews in biomedical engineering*, 9:32–48, 2016.

[4] Patrick L Reavey, John T Stranix, Horatiu Muresan, Marc Soares, and Vishal Thanik. Disappearing digits: Analysis of national trends in amputation and replantation in the united states. *Plastic and Reconstructive Surgery*, 141(6):857e–867e, 2018.

[5] Adenike A Adewuyi, Levi J Hargrove, and Todd A Kuiken. Towards improved partial-hand prostheses: The effect of wrist kinematics on pattern-recognition-based control. In *Neural Engineering (NER), 2013 6th International IEEE/EMBS Conference on*, pages 1489–1492. IEEE, 2013.

[6] MS Lynsay Whelan, LPO Nathan Wagner, et al. Individualizing goals for users of externally powered partial hand prostheses. *Journal of rehabilitation research and development*, 51(6):885, 2014.

[7] Robert D. Rondinelli, Christopher R. Brigham, Elizabeth Genovese, et al. *Guides to the evaluation of permanent impairment.* 6th ed. / medical editor, robert d. rondinelli ; section editors, elizabeth genovese [and others] ; senior contributing editor, christopher r. brigham. edition, 2008. ISBN 1579478883.

[8] Helena Burger, Tomaž Maver, and Črt Marinček. Partial hand amputation and work. *Disability and rehabilitation*, 29(17):1317–1321, 2007.

[9] Bartjan Maat, Gerwin Smit, Dick Plettenburg, and Paul Breedveld. Passive prosthetic hands and tools: A literature review. *Prosthetics and orthotics international*, page 0309364617691622, 2017.

[10] Kai Xu, Huan Liu, Zhaoyu Zhang, and Xiangyang Zhu. Wrist-powered partial hand prosthesis using a continuum whiffle tree mechanism: A case study. *IEEE Transactions on Neural Systems and Rehabilitation Engineering*, 26(3):609–618, 2018.

[11] Lynsay R Whelan and Jeremy Farley. Functional outcomes with externally powered partial hand prostheses. *JPO: Journal of Prosthetics and Orthotics*, 30(2):69–73, 2018.

[12] Agamemnon Krasoulis, Student Member, and Sethu Vijayakumar. Evaluation of Regression Methods for the Continuous Decoding of Finger Movement from Surface EMG and Accelerometry. In *7th Annual International IEEE EMBS Conference on Neural Engineering*, pages 631–634, Montpellier, 2015. ISBN 9781467363891.

[13] Zhen G Xiao and Carlo Menon. Towards the development of a wearable feedback system for monitoring the activities of the upper-extremities. *Journal of neuroengineering and rehabilitation*, 11(1):2, 2014.

[14] Adenike A Adewuyi, Levi J Hargrove, and Todd A Kuiken. Resolving the effect of wrist position on myoelectric pattern recognition control. *Journal of neuroengineering and rehabilitation*, 14(1):39, 2017.

[15] Eric J Earley, Adenike A Adewuyi, and Levi J Hargrove. Optimizing pattern recognition-based control for partial-hand prosthesis application. In *Engineering in Medicine and Biology Society (EMBC), 2014 36th Annual International Conference of the IEEE*, pages 3574–3577. IEEE, 2014.

[16] Keith L Moore. *Clinically oriented anatomy.* The Williams & Wilkins Co., 1980.

[17] Keith L Moore, Arthur F Dalley, and Anne MR Agur. *Clinically oriented anatomy.* Lippincott Williams & Wilkins, 2013.

[18] Claudio Castellini, Georg Passig, and Emanuel Zarka. Using ultrasound images of the forearm to predict finger positions. *IEEE Transactions on Neural Systems and Rehabilitation Engineering*, 20(6):788–797, 2012.

[19] David Sierra González and Claudio Castellini. A realistic implementation of ultrasound imaging as a human-machine interface for upper-limb amputees. *Frontiers in neurorobotics*, 7:17, 2013.

[20] Siddhartha Sikdar, Huzefa Rangwala, Emily B Eastlake, Ira A Hunt, Andrew J Nelson, Jayanth Devanathan, Andrew Shin, and Joseph J Pancrazio. Novel method for predicting dexterous individual finger movements by imaging muscle activity using a wearable ultrasonic system. *IEEE Transactions on Neural Systems and Rehabilitation Engineering*, 22(1):69–76, 2014.

[21] Barys Ihnatsenka and André Pierre Boezaart. Ultrasound: Basic understanding and learning the language. *International journal of shoulder surgery*, 4(3):55, 2010.

[22] Valerio Ortenzi, Sergio Tarantino, Claudio Castellini, and Christian Cipriani. Ultrasound imaging for hand prosthesis control: a comparative study of features and classification methods. In *Rehabilitation Robotics (ICORR), 2015 IEEE International Conference on*, pages 1–6. IEEE, 2015.

[23] Nima Akhlaghi, Clayton A Baker, Mohamed Lahlou, Hozaifah Zafar, Karthik G Murthy, Huzefa S Rangwala, Jana Kosecka, Wilsaan M Joiner, Joseph J Pancrazio, and Siddhartha Sikdar. Real-time classification of hand motions using ultrasound imaging of forearm muscles. *IEEE Transactions on Biomedical Engineering*, 63(8):1687–1698, 2016.

[24] Clayton A Baker, Nima Akhlaghi, Huzefa Rangwala, Jana Kosecka, and Siddhartha Sikdar. Real-time, ultrasound-based control of a virtual hand by a trans-radial amputee. In *Engineering in Medicine and Biology Society (EMBC), 2016 IEEE 38th Annual International Conference of the*, pages 3219–3222. IEEE, 2016.

[25] Christian Nissler, Nikoleta Mouriki, Claudio Castellini, Vasileios Belagiannis, and Nassir Navab. Omg: introducing optical myography as a new human machine interface for hand amputees. In *Rehabilitation Robotics (ICORR), 2015 IEEE International Conference on*, pages 937–942. IEEE, 2015.

[26] Yu Tzu Wu, Eric Fujiwara, and Carlos K Suzuki. Optical myography system for posture monitoring. In *Consumer Electronics (ISCE), 2016 IEEE International Symposium on*, pages 37–38. IEEE, 2016.

[27] Ryan J Smith, Francesco Tenore, David Huberdeau, Ralph Etienne-Cummings, and Nitish V Thakor. Continuous decoding of finger position from surface emg signals for the control of powered prostheses. In *Engineering in Medicine and Biology Society, 2008. EMBS 2008. 30th Annual International Conference of the IEEE*, pages 197–200. IEEE, 2008.

[28] Jimson Ngeo, Tomoya Tamei, and Tomohiro Shibata. Continuous estimation of finger joint angles using muscle activation inputs from surface emg signals. In *Engineering in Medicine and Biology Society (EMBC), 2012 Annual International Conference of the IEEE*, pages 2756–2759. IEEE, 2012.

[29] Lizhi Pan, Xinjun Sheng, Dingguo Zhang, and Xiangyang Zhu. Simultaneous and proportional estimation of finger joint angles from surface emg signals during mirrored bilateral movements. In *International Conference on Intelligent Robotics and Applications*, pages 493–499. Springer, 2013.

[30] Lizhi Pan, Dingguo Zhang, Jianwei Liu, Xinjun Sheng, and Xiangyang Zhu. Continuous estimation of finger joint angles under different static wrist motions from surface emg signals. *Biomedical Signal Processing and Control*, 14:265–271, 2014.

[31] Zhen Gang Xiao and Carlo Menon. Counting grasping action using force myography: An exploratory study with healthy individuals. *JMIR Rehabilitation and Assistive Technologies*, 4(1), 2017.

[32] Claudio Castellini, Panagiotis Artemiadis, Michael Wininger, Arash Ajoudani, Merkur Alimusaj, Antonio Bicchi, Barbara Caputo, William Craelius, Strahinja Dosen, Kevin Englehart, et al. Proceedings of the first workshop on peripheral machine interfaces: Going beyond traditional surface electromyography. *Frontiers in neurorobotics*, 8, 2014.

[33] Michael Wininger, Nam-Hun Kim, and William Craelius. Pressure signature of forearm as predictor of grip force. *Journal of rehabilitation research and development*, 45(6): 883–892, 2008.

[34] Sam L Phillips and William Craelius. Residual kinetic imaging: a versatile interface for prosthetic control. *Robotica*, 23(3):277–282, 2005.

[35] Samuel Lon Phillips. *Residual kinetics indices: A versatile interface for prosthetic control*. Rutgers The State University of New Jersey-New Brunswick and University of Medicine and Dentistry of New Jersey, 2007.

[36] Nan Li, Dapeng Yang, Li Jiang, Hong Liu, and Hegao Cai. Combined use of fsr sensor array and svm classifier for finger motion recognition based on pressure distribution map. *Journal of Bionic Engineering*, 9(1):39–47, 2012.

[37] Mathilde Connan, Eduardo Ruiz Ramírez, Bernhard Vodermayer, and Claudio Castellini. Assessment of a wearable force-and electromyography device and comparison of the related signals for myocontrol. *Frontiers in neurorobotics*, 10:17, 2016.

[38] Erina Cho, Richard Chen, Lukas-Karim Merhi, Zhen Xiao, Brittany Pousett, and Carlo Menon. Force myography to control robotic upper extremity prostheses: a feasibility study. *Frontiers in bioengineering and biotechnology*, 4:18, 2016.

[39] Xianta Jiang, Lukas-Karim Merhi, Zhen Gang Xiao, and Carlo Menon. Exploration of force myography and surface electromyography in hand gesture classification. *Medical Engineering and Physics*, 41:63–73, 2017.

[40] Claudio Castellini and Vikram Ravindra. A wearable low-cost device based upon force-sensing resistors to detect single-finger forces. In *Biomedical Robotics and Biomechatronics (2014 5th IEEE RAS & EMBS International Conference on*, pages 199–203. IEEE, 2014.

[41] Maram Sakr and Carlo Menon. Regressing force-myographic signals collected by an armband to estimate torque exerted by the wrist: A preliminary investigation. In *Electrical and Computer Engineering (CCECE), 2016 IEEE Canadian Conference on*, pages 1–4. IEEE, 2016.

[42] Maram Sakr and Carlo Menon. On the estimation of isometric wrist/forearm torque about three axes using force myography. In *Biomedical Robotics and Biomechatronics (BioRob), 2016 6th IEEE International Conference on*, pages 827–832. IEEE, 2016.

[43] Anders Fougner, Erik Scheme, Adrian DC Chan, Kevin Englehart, and Øyvind Stavdahl. Resolving the limb position effect in myoelectric pattern recognition. *IEEE Transactions on Neural Systems and Rehabilitation Engineering*, 19(6):644–651, 2011.

[44] Ashkan Radmand, Erik Scheme, and Kevin Englehart. High-density force myography: A possible alternative for upper-limb prosthetic control. *Journal of Rehabilitation Research & Development*, 53(4), 2016.

[45] Anita Kadkhodayan, Xianta Jiang, and Carlo Menon. Continuous prediction of finger movements using force myography. *Journal of Medical and Biological Engineering*, 36 (4):594–604, 2016.

[46] Christopher M Bishop. *Pattern Recognition and Machine Learning*. Springer-Verlag New York, 2006.

[47] Zhen Gang Xiao and Carlo Menon. Performance of forearm fmg and semg for estimating elbow, forearm and wrist positions. *Journal of Bionic Engineering*, 14(2):284–295, 2017.

[48] Antje Kirchner and Curtis S Signorino. Using support vector machines for survey research. *Survey Practice*, 11(1), 2018.

[49] Leo Breiman. Random forests. *Machine learning*, 45(1):5–32, 2001.

[50] Andy Liaw, Matthew Wiener, et al. Classification and regression by randomforest. *R news*, 2(3):18–22, 2002.

[51] Gautam P Sadarangani and Carlo Menon. A preliminary investigation on the utility of temporal features of force myography in the two-class problem of grasp vs. no-grasp in the presence of upper-extremity movements. *Biomedical engineering online*, 16(1): 59, 2017.

[52] Rana Sadeghi Chegani, Mona L Delva, Maram Sakr, Carlo Menon, et al. Pilot study on strategies in sensor placement for robust hand/wrist gesture classification based on movement related changes in forearm volume. In *Healthcare Innovation Point-Of-Care Technologies Conference (HI-POCT), 2016 IEEE*, pages 46–49. IEEE, 2016.

[53] *FSR® 400 Series datasheet*. Interlink Electronics, .

[54] *FSR® Integration Guide*. Interlink Electronics, . Rev. C.

[55] Zhen Gang Xiao. *Detecting upper extremity activity with force myography*. PhD thesis, Applied Sciences: School of Engineering Science, 2017.

[56] Dena Senior. Qualisys track manager: User manual. 2004.

[57] Mark R Cutkosky. On grasp choice, grasp models, and the design of hands for manufacturing tasks. *IEEE Transactions on robotics and automation*, 5(3):269–279, 1989.

[58] Loredana Zollo, Stefano Roccella, Eugenio Guglielmelli, M Chiara Carrozza, and Paolo Dario. Biomechatronic design and control of an anthropomorphic artificial hand for prosthetic and robotic applications. *IEEE/ASME Transactions On Mechatronics*, 12 (4):418–429, 2007.

[59] Mariangela Manti, Taimoor Hassan, Giovanni Passetti, Nicolò D'Elia, Cecilia Laschi, and Matteo Cianchetti. A Bioinspired Soft Robotic Gripper for Adaptable and Effective Grasping. *Soft Robotics*, 2(3):107–116, 2015. ISSN 2169-5172.

[60] H Jiang, J P Wachs, and B S Duerstock. Integrated vision-based robotic arm interface for operators with upper limb mobility impairments. In *2013 IEEE 13th International Conference on Rehabilitation Robotics (ICORR)*, pages 1–6, Seattle, 2013. ISBN 1945-7898 VO -.

[61] James L Rogers, Kenneth I Howard, and John T Vessey. Using significance tests to evaluate equivalence between two experimental groups. *Psychological bulletin*, 113(3): 553, 1993.

Appendix A

A.1 Removing different wrist positions from training data set

This section will provide the results of removing different wrist positions. Each table provides the average results of the removing wrist positions among participants and repetitions. Tables A.1 and A.2 indicate the results of removing one wrist position from the training data set. Tables A.3 and A.4 indicate the results of removing two wrist positions from the training data set. Tables A.5 and A.6 indicate the results of removing three wrist positions from the training data set. Tables A.7 and A.8 indicate the results of removing four wrist positions from the training data set. Tables A.9 and A.10 indicate the results of removing five wrist positions from the training data set.

Table A.1: The result of removing one wrist positions from training data, θ_{TI}

Removed Wrist Position	R^2	RMSE%
Extension	0.8209 ± 0.0564	$11.07 \pm 1.37\%$
Flexion	0.8002 ± 0.0662	$11.69 \pm 1.82\%$
Neutral	0.7940 ± 0.0603	$11.93 \pm 1.65\%$
Pronation	0.8418 ± 0.0460	$10.43 \pm 1.36\%$
Radial	0.8450 ± 0.0465	$10.32 \pm 1.34\%$
Ulnar	0.8325 ± 0.0513	$10.72 \pm 1.24\%$

A.2 Full Results of the statistical analyses of the Effect of the Wrist Position variation

Each option for removing one or more wrist positions is identified with a group number. The case of including all wrist positions in the training data set is identified as "group 1".

Table A.2: The result of removing one wrist positions from training data, θ_{TM}

Removed Wrist Position	R^2	RMSE%
Extension	0.9014 ± 0.0511	7.81 ± 1.57%
Flexion	0.8955 ± 0.038	8.19 ± 1.11%
Neutral	0.8736 ± 0.0676	8.85 ± 2.22%
Pronation	0.9274 ± 0.0337	6.75 ± 1.22%
Radial	0.9254 ± 0.0394	6.80 ± 1.19%
Ulnar	0.9158 ± 0.0387	7.24 ± 1.07%

Figures A.1 - A.4 indicate the pairwise comparison of the different options for training data set. The figures can indicate the overlapping options. We can not establish any statistically significant difference between the options that have an overlapping interval. Table A.11 indicates the removed wrist positions and their group id.

A.3 Snap Shot of Hand Movement Signal in Different Wrist Positions

This section a sample of the FMG signal in different hand movements and wrist positions. The graphs from top to bottom show the opposed Thumb-Index finger grip, opposed Thumb-Two finger grip, and oppose Heavy Wrap. The sections of the graphs that are number as 1-6 indicate the Extension wrist position, Flexion wrist position, Neutral wrist position, Pronation wrist position, Radial wrist position and Ulnar wrist position. Different colors on the graph indicate the different sensor values.

Table A.3: The result of removing two wrist positions from training data, θ_{TI}

Removed Wrist Positions	R^2	RMSE%
Extension and Flexion	0.7506 ± 0.08	13.10 ± 2.07%
Extension and Neutral	0.6914 ± 0.11	14.46 ± 2.24%
Extension and Pronation	0.7882 ± 0.08	12.00 ± 1.89%
Extension and Radial	0.7957 ± 0.07	11.82 ± 1.58%
Extension and Ulnar	0.7603 ± 0.09	12.77 ± 1.98%
Flexion and Neutral	0.7270 ± 0.08	13.75 ± 1.90%
Flexion and Pronation	0.7803 ± 0.07	12.27 ± 1.86%
Flexion and Radial	0.7638 ± 0.09	12.64 ± 2.10%
Flexion and Ulnar	0.7621 ± 0.08	12.73 ± 1.90%
Neutral and Pronation	0.7605 ± 0.06	12.88 ± 1.63%
Neutral and Radial	0.7671 ± 0.07	12.69 ± 1.76%
Neutral and Ulnar	0.7565 ± 0.07	12.96 ± 1.64%
Pronation and Radial	0.7696 ± 0.09	12.51 ± 2.43%
Pronation and Ulnar	0.7868 ± 0.06	12.13 ± 1.39%
Radial and Ulnar	0.8012 ± 0.07	11.66 ± 1.64%

Table A.4: The result of removing two wrist positions from training data, θ_{TM}

Removed Wrist Positions	R^2	RMSE%
Extension and Flexion	0.8571 ± 0.06	9.52 ± 1.69%
Extension and Neutral	0.7910 ± 0.12	11.36 ± 2.40%
Extension and Pronation	0.8816 ± 0.07	8.44 ± 2.07%
Extension and Radial	0.8867 ± 0.06	8.35 ± 1.68%
Extension and Ulnar	0.8533 ± 0.09	9.42 ± 2.26%
Flexion and Neutral	0.8527 ± 0.06	9.71 ± 1.86%
Flexion and Pronation	0.8815 ± 0.05	8.66 ± 1.38%
Flexion and Radial	0.8776 ± 0.05	8.82 ± 1.31%
Flexion and Ulnar	0.8714 ± 0.06	8.95 ± 1.34%
Neutral and Pronation	0.8595 ± 0.07	9.35 ± 2.16%
Neutral and Radial	0.8614 ± 0.08	9.23 ± 2.30%
Neutral and Ulnar	0.8457 ± 0.08	9.80 ± 2.0%
Pronation and Radial	0.8764 ± 0.08	8.58 ± 2.46%
Pronation and Ulnar	0.8983 ± 0.05	7.96 ± 1.23%
Radial and Ulnar	0.8979 ± 0.06	7.90 ± 1.43%

Table A.5: The result of removing three wrist positions from training data, θ_{TI}

Removed Wrist Positions	R2	RMSE%
Extension and Flexion and Neutral	0.6328 ± 0.13	15.85 ± 2.49%
Extension and Flexion and Pronation	0.7252 ± 0.09	13.76 ± 2.11%
Extension and Flexion and Radial	0.7125 ± 0.10	14.00 ± 2.22%
Extension and Flexion and Ulnar	0.7002 ± 0.10	14.33 ± 2.30%
Extension and Neutral and Pronation	0.6526 ± 0.13	15.33 ± 2.48%
Extension and Neutral and Radial	0.6650 ± 0.12	15.08 ± 2.34%
Extension and Neutral and Ulnar	0.6163 ± 0.16	16.06 ± 2.78%
Extension and Pronation and Radial	0.7216 ± 0.12	13.71 ± 2.65%
Extension and Pronation and Ulnar	0.7090 ± 0.10	14.12 ± 2.18%
Extension and Radial and Ulnar	0.7313 ± 0.10	13.52 ± 2.32%
Flexion and Neutral and Pronation	0.7075 ± 0.08	14.22 ± 2.00%
Flexion and Neutral and Radial	0.6904 ± 0.10	14.58 ± 2.11%
Flexion and Neutral and Ulnar	0.6910 ± 0.09	14.58 ± 1.98%
Flexion and Pronation and Radial	0.7103 ± 0.10	14.05 ± 2.37%
Flexion and Pronation and Ulnar	0.7277 ± 0.09	13.65 ± 1.98%
Flexion and Radial and Ulnar	0.7301 ± 0.10	13.55 ± 2.06%
Neutral and Pronation and Radial	0.6939 ± 0.10	14.53 ± 2.24%
Neutral and Pronation and Ulnar	0.7098 ± 0.07	14.19 ± 1.60 %
Neutral and Radial and Ulnar	0.7290 ± 0.08	13.68 ± 1.79%
Pronation and Radial and Ulnar	0.5342 ± 0.21	17.60 ± 3.55%

Table A.6: The result of removing three wrist positions from training data, θ_{TM}

Removed Wrist Positions	R^2	RMSE%
Extension and Flexion and Neutral	0.7591 ± 0.15	12.07 ± 2.70%
Extension and Flexion and Pronation	0.8408 ± 0.07	9.98 ± 1.91%
Extension and Flexion and Radial	0.8394 ± 0.07	10.09 ± 1.72%
Extension and Flexion and Ulnar	0.8084 ± 0.08	10.99 ± 1.88%
Extension and Neutral and Pronation	0.7672 ± 0.13	11.95 ± 2.53%
Extension and Neutral and Radial	0.7789 ± 0.12	11.71 ± 2.38%
Extension and Neutral and Ulnar	0.6988 ± 0.19	13.43 ± 3.68%
Extension and Pronation and Radial	0.8455 ± 0.09	9.67 ± 2.28%
Extension and Pronation and Ulnar	0.8289 ± 0.10	10.19 ± 2.36%
Extension and Radial and Ulnar	0.8363 ± 0.10	9.94 ± 2.41%
Flexion and Neutral and Pronation	0.8337 ± 0.06	10.32 ± 1.84%
Flexion and Neutral and Radial	0.8359 ± 0.07	10.21 ± 1.95%
Flexion and Neutral and Ulnar	0.8283 ± 0.07	10.42 ± 1.85%
Flexion and Pronation and Radial	0.8205 ± 0.09	10.60 ± 2.32%
Flexion and Pronation and Ulnar	0.8541 ± 0.08	9.51 ± 1.55%
Flexion and Radial and Ulnar	0.8513 ± 0.08	9.62 ± 1.57%
Neutral and Pronation and Radial	0.8161 ± 0.12	10.54 ± 2.71%
Neutral and Pronation and Ulnar	0.8310 ± 0.07	10.36 ± 1.72%
Neutral and Radial and Ulnar	0.8316 ± 0.09	10.19 ± 2.18%
Pronation and Radial and Ulnar	0.7021 ± 0.22	12.94 ± 4.20%

Table A.7: The result of removing four wrist positions from training data, θ_{TI}

Removed Wrist Positions	R^2	RMSE%
Extension and Flexion and Neutral and Pronation	0.6068 ± 0.15	16.33 ± 2.65%
Extension and Flexion and Neutral and Radial	0.5947 ± 0.15	16.62 ± 2.79%
Extension and Flexion and Neutral and Ulnar	0.5857 ± 0.15	16.80 ± 2.57%
Extension and Flexion and Pronation and Radial	0.6540 ± 0.12	15.38 ± 2.46%
Extension and Flexion and Pronation and Ulnar	0.6591 ± 0.11	15.32 ± 2.40%
Extension and Flexion and Radial and Ulnar	0.6686 ± 0.11	15.08 ± 2.41%
Extension and Neutral and Pronation and Radial	0.5967 ± 0.15	16.59 ± 2.68%
Extension and Neutral and Pronation and Ulnar	0.5445 ± 0.20	17.47 ± 3.29%
Extension and Neutral and Radial and Ulnar	0.5855 ± 0.16	16.75 ± 2.85%
Extension and Pronation and Radial and Ulnar	0.4303 ± 0.26	19.52 ± 4.12%
Flexion and Neutral and Pronation and Radial	0.6337 ± 0.13	15.82 ± 2.51%
Flexion and Neutral and Pronation and Ulnar	0.6568 ± 0.11	15.36 ± 2.15%
Flexion and Neutral and Radial and Ulnar	0.6637 ± 0.10	15.21 ± 2.10%
Flexion and Pronation and Radial and Ulnar	0.4862 ± 0.20	18.59 ± 2.92%
Neutral and Pronation and Radial and Ulnar	0.4582 ± 0.20	19.19 ± 3.01%

Table A.8: The result of removing four wrist positions from training data, θ_{TM}

Removed Wrist Positions	R^2	RMSE%
Extension and Flexion and Neutral and Pronation	0.7172 ± 0.18	12.99 ± 2.88%
Extension and Flexion and Neutral and Radial	0.7551 ± 0.12	12.33 ± 2.50%
Extension and Flexion and Neutral and Ulnar	0.6937 ± 0.19	13.61 ± 3.12%
Extension and Flexion and Pronation and Radial	0.7809 ± 0.10	11.73 ± 2.31%
Extension and Flexion and Pronation and Ulnar	0.7869 ± 0.09	11.61 ± 1.93%
Extension and Flexion and Radial and Ulnar	0.7889 ± 0.09	11.54 ± 2.05%
Extension and Neutral and Pronation and Radial	0.7413 ± 0.16	12.55 ± 2.64%
Extension and Neutral and Pronation and Ulnar	0.6459 ± 0.23	14.57 ± 4.03%
Extension and Neutral and Radial and Ulnar	0.6866 ± 0.20	13.76 ± 3.65%
Extension and Pronation and Radial and Ulnar	0.6494 ± 0.17	14.63 ± 3.08%
Flexion and Neutral and Pronation and Radial	0.7805 ± 0.11	11.71 ± 2.43%
Flexion and Neutral and Pronation and Ulnar	0.8045 ± 0.08	11.10 ± 1.94%
Flexion and Neutral and Radial and Ulnar	0.8113 ± 0.09	10.87 ± 2.03%
Flexion and Pronation and Radial and Ulnar	0.6243 ± 0.27	14.65 ± 4.21%
Neutral and Pronation and Radial and Ulnar	0.6518 ± 0.22	14.40 ± 3.27%

Table A.9: The result of removing five wrist positions from training data, θ_{TI}

Removed Wrist Positions	R^2	RMSE%
Extension and Flexion and Neutral and Pronation and Radial	0.5022 ± 0.28	18.10 ± 3.66%
Extension and Flexion and Neutral and Pronation and Radial	0.5534 ± 0.16	17.45 ± 2.60%
Extension and Flexion and Neutral and Radial and Ulnar	0.5501 ± 0.16	17.56 ± 2.73%
Extension and Flexion and Pronation and Radial and Ulnar	0.3724 ± 0.21	20.70 ± 3.50%
Extension and Neutral and Pronation and Radial and Ulnar	0.2308 ± 0.34	22.64 ± 4.16%
Flexion and Neutral and Pronation and Radial and Ulnar	0.4106 ± 0.23	19.90 ± 2.79%

Table A.10: The result of removing five wrist positions from training data, θ_{TM}

Removed Wrist Positions	R2	RMSE%
Extension and Flexion and Neutral and Pronation and Radial	0.6409 + 0.28	14.42 + 3.55%
Extension and Flexion and Neutral and Pronation and Radial	0.6311 + 0.20	15.03 + 3.30%
Extension and Flexion and Neutral and Radial and Ulnar	0.7003 + 0.17	13.53 + 2.92%
Extension and Flexion and Pronation and Radial and Ulnar	0.5931 + 0.16	16.07 + 2.82%
Extension and Neutral and Pronation and Radial and Ulnar	0.4356 + 0.34	18.36 + 4.01%
Flexion and Neutral and Pronation and Radial and Ulnar	0.5660 + 0.30	15.74 + 4.46%

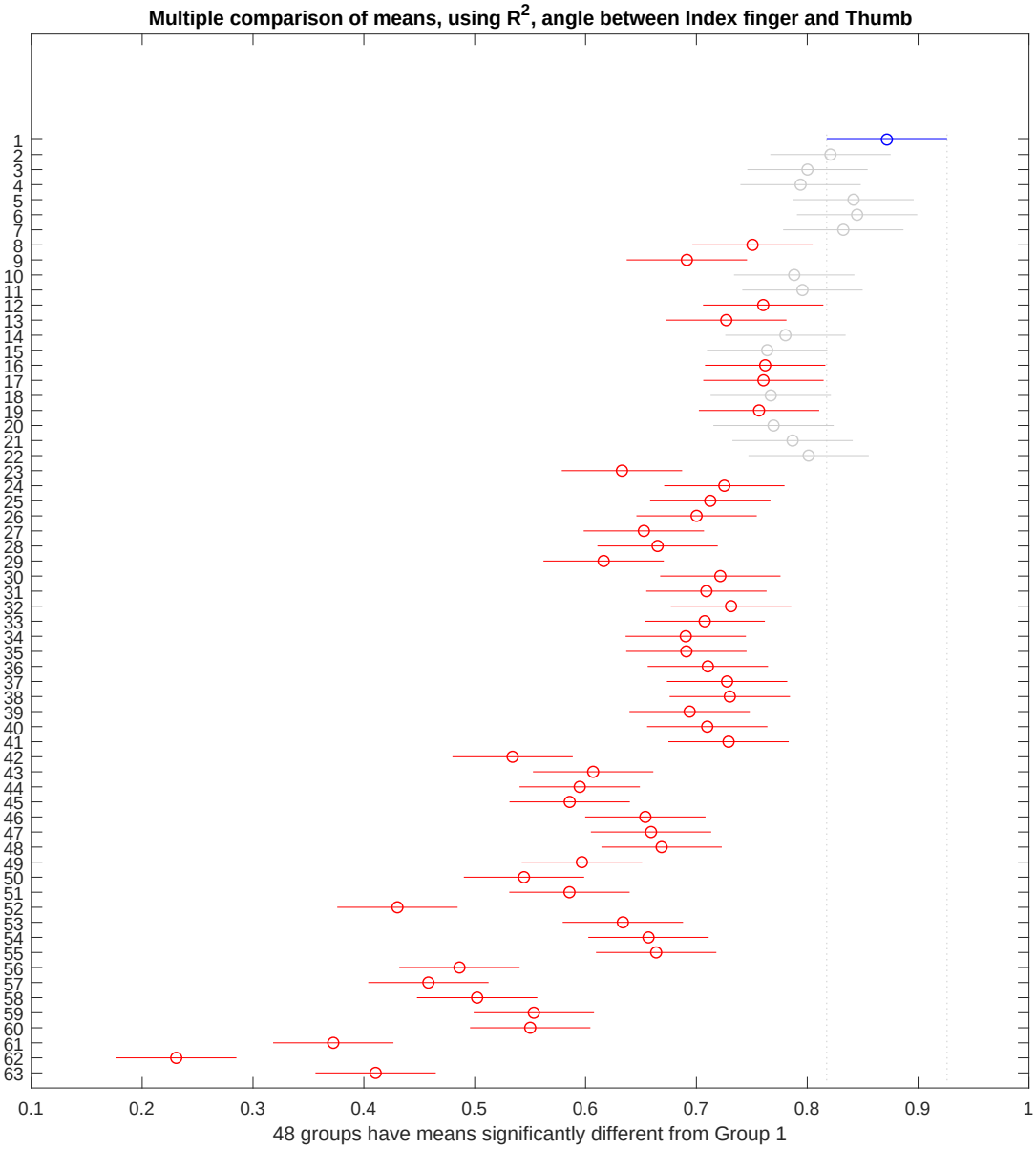

Figure A.1: The multiple comparison of mean, using R^2, θ_{TI}

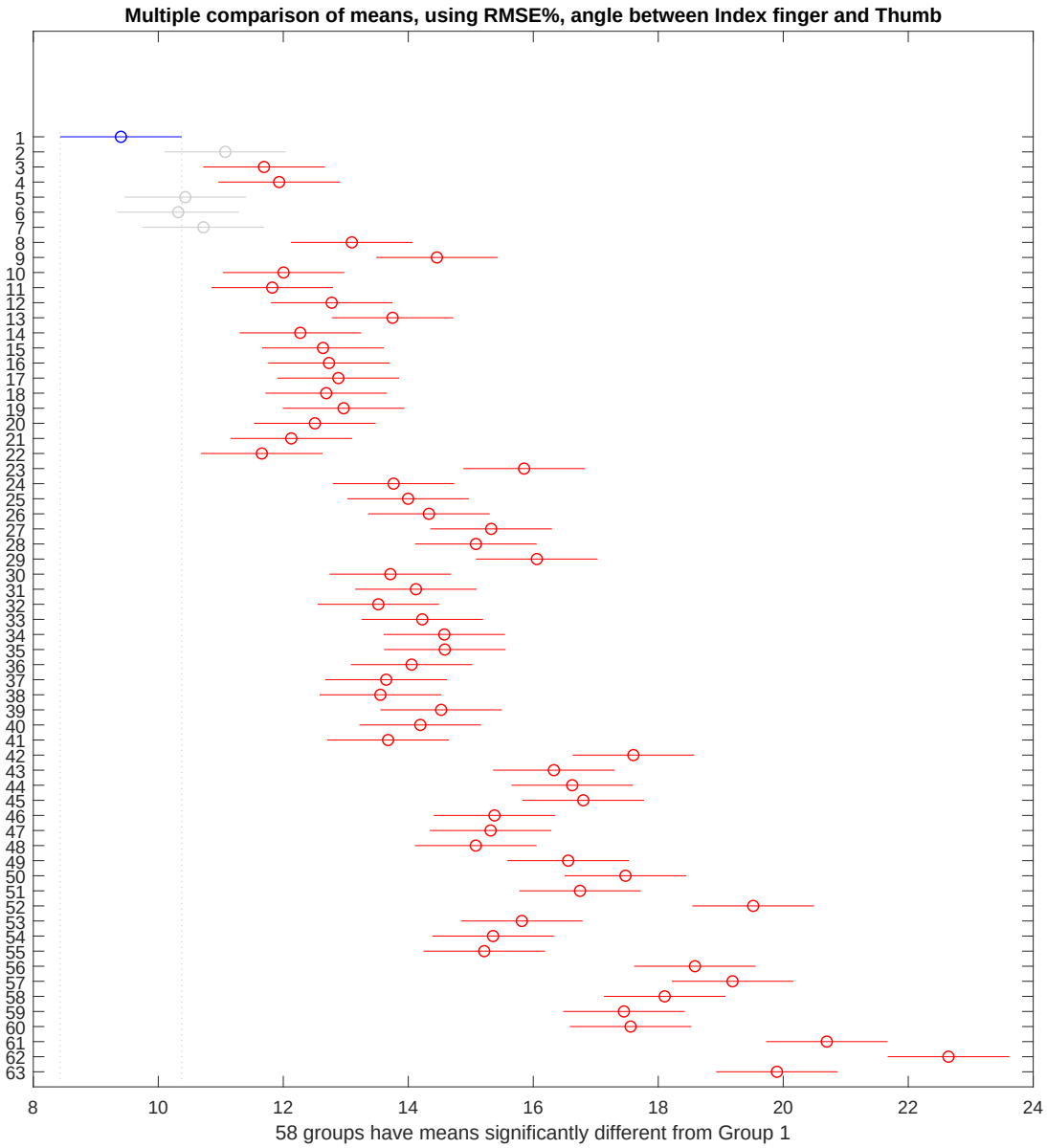

Figure A.2: The multiple comparison of mean, using $RMSE\%$, θ_{TI}

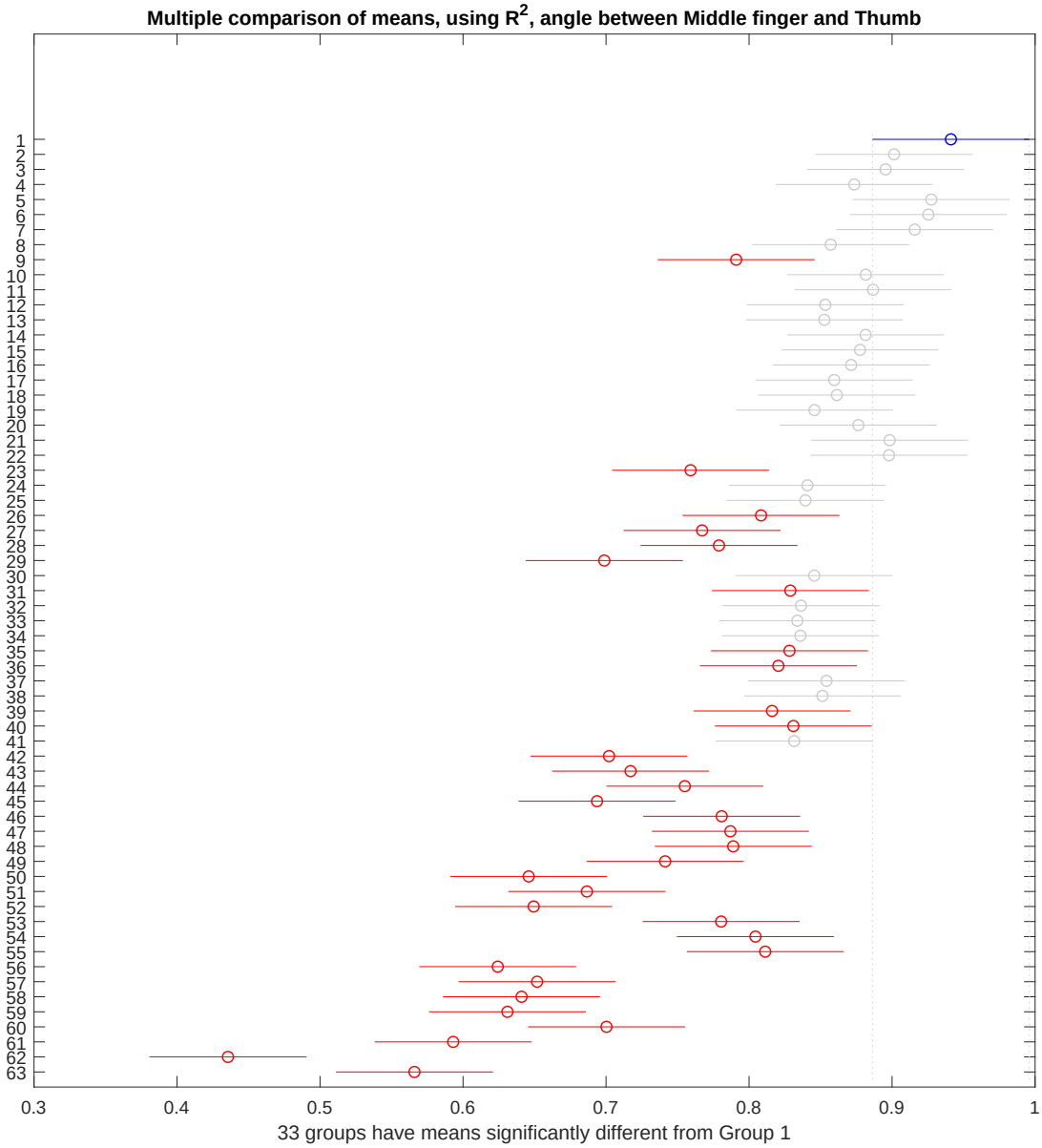

Figure A.3: The multiple comparison of mean, using R^2, θ_{TM}

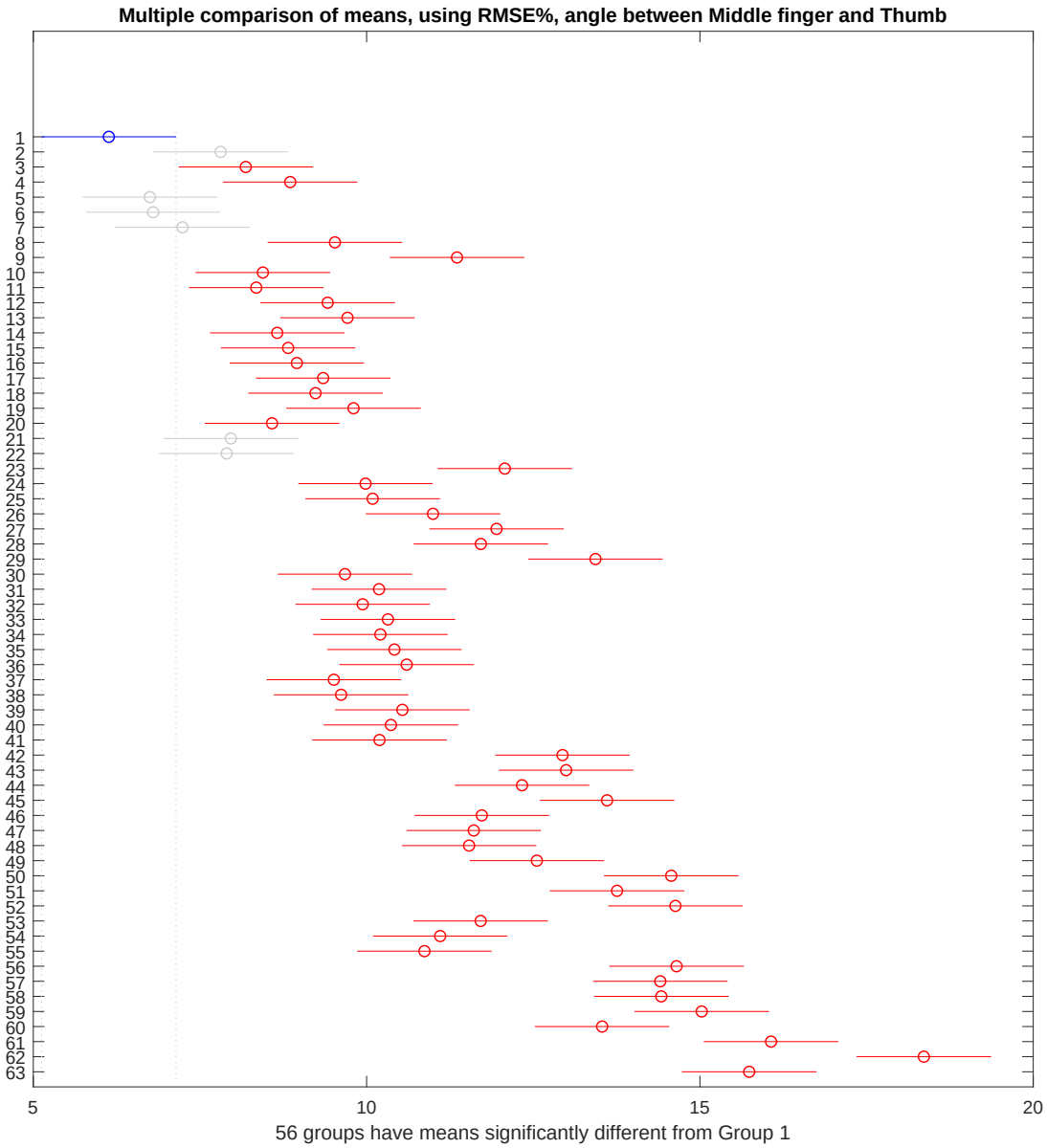

Figure A.4: The multiple comparison of mean, using $RMSE\%$, θ_{TM}

Table A.11: Removed wrist positions and their group id

group id	removed wrist positions	group id	removed wrist positions	group id	removed wrist positions
1	None	22	Radial, Ulnar	43	Extension, Flexion, Neutral, Pronation
2	Extension	23	Extension, Flexion, Neutral	44	Extension, Flexion, Neutral, Radial
3	Flexion	24	Extension, Flexion, Pronation	45	Extension, Flexion, Neutral, Ulnar
4	Neutral	25	Extension, Flexion, Radial	46	Extension, Flexion, Pronation, Radial
5	Pronation	26	Extension, Flexion, Ulnar	47	Extension, Flexion, Pronation, Ulnar
6	Radial	27	Extension, Neutral, Pronation	48	Extension, Flexion, Radial, Ulnar
7	Ulnar	28	Extension, Neutral, Radial	49	Extension, Neutral, Pronation, Radial
8	Extension, Flexion	29	Extension, Neutral, Ulnar	50	Extension, Neutral, Pronation, Ulnar
9	Extension, Neutral	30	Extension, Pronation, Radial	51	Extension, Neutral, Radial, Ulnar
10	Extension, Pronation	31	Extension, Pronation, Ulnar	52	Extension, Pronation, Radial, Ulnar
11	Extension, Radial	32	Extension, Radial, Ulnar	53	Flexion, Neutral, Pronation, Radial
12	Extension, Ulnar	33	Flexion, Neutral, Pronation	54	Flexion, Neutral, Pronation, Ulnar
13	Flexion, Neutral	34	Flexion, Neutral, Radial	55	Flexion, Neutral, Radial, Ulnar
14	Flexion, Pronation	35	Flexion, Neutral, Ulnar	56	Flexion, Pronation, Radial, Ulnar
15	Flexion, Radial	36	Flexion, Pronation, Radial	57	Neutral, Pronation, Radial, Ulnar
16	Flexion, Ulnar	37	Flexion, Pronation, Ulnar	58	Extension, Flexion, Neutral, Pronation
17	Neutral, Pronation	38	Flexion, Radial, Ulnar	59	Extension, Flexion, Neutral, Pronation
18	Neutral, Radial	39	Neutral, Pronation, Radial	60	Extension, Flexion, Neutral, Radial, Ulnar
19	Neutral, Ulnar	40	Neutral, Pronation, Ulnar	61	Extension, Flexion, Pronation, Radial, Ulnar
20	Pronation, Radial	41	Neutral, Radial, Ulnar	62	Extension, Neutral, Pronation, Radial, Ulnar
21	Pronation, Ulnar	42	Pronation, Radial, Ulnar	63	Flexion, Neutral, Pronation, Radial, Ulnar

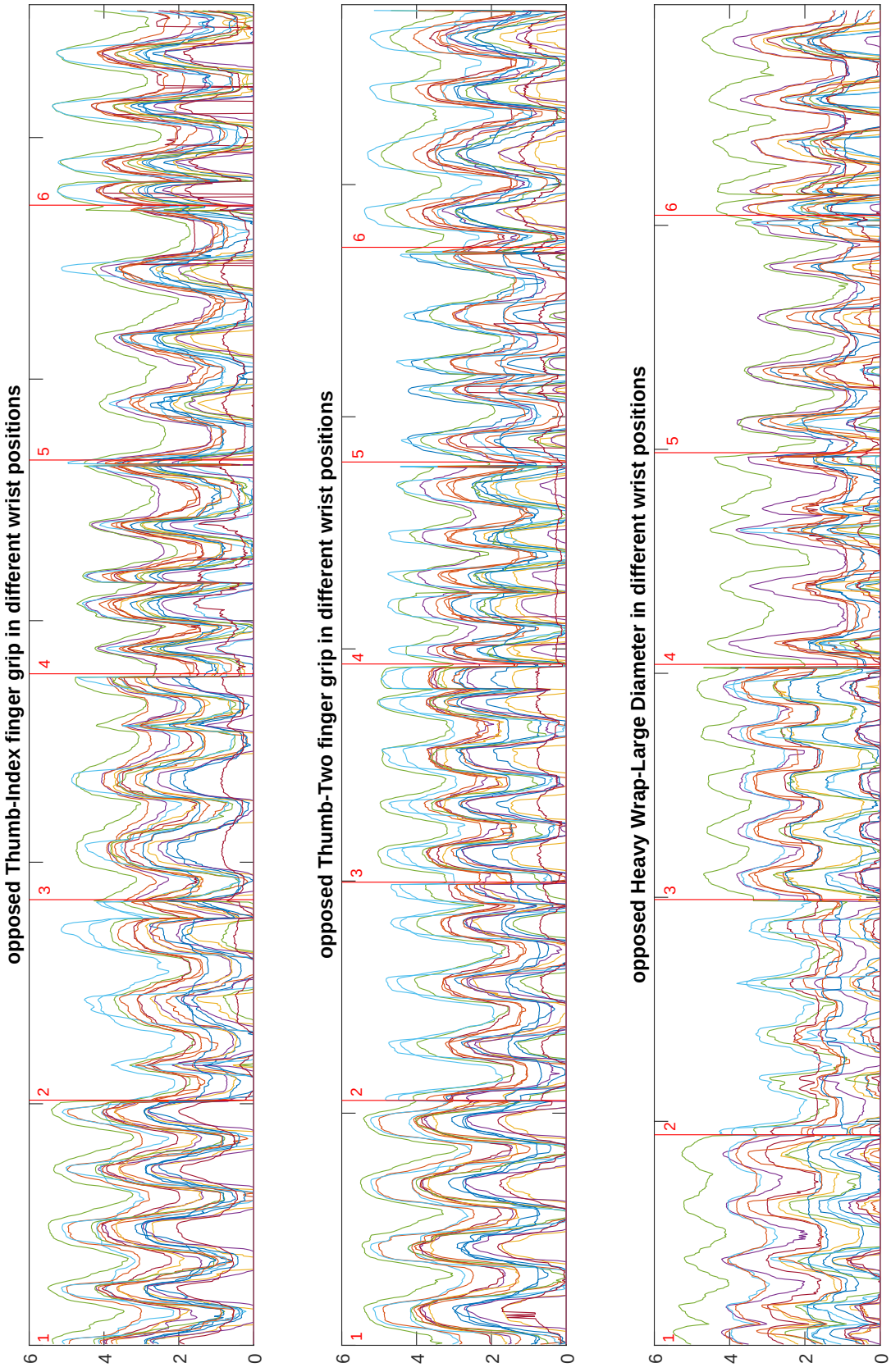

Figure A.5: Comparison between the FMG signal in different wrist positions